國立臺灣大學生命科學院基因體與系統生物學學位學程

博士論文

Genome and Systems Biology Degree Program

College of Life Science

National Taiwan University

Doctoral Dissertation

全面性分析在自閉症表現量異常的環狀核糖核酸及環狀核糖核酸–微小核糖核酸–信使核糖核酸間相互調控網路

Integrative analysis of circular RNA dysregulation and circular RNA-microRNA-mRNA regulatory axes in autism

陳彥如

Yen-Ju Chen

指導教授: 莊樹諄 博士

Advisor: Trees-Juen Chuang, Ph.D.

中華民國 109 年 5 月

May 2020

doi:10.6342/NTU202000765

口試委員審定書

國立臺灣大學博士學位論文
口試委員會審定書

全面性分析在自閉症表現量異常的環狀核糖核酸及環狀核糖核酸–微小核糖核酸–信使核糖核酸間相互調控網路

Integrative analysis of circular RNA dysregulation and circular RNA-microRNA-mRNA regulatory axes in autism

本論文係 陳彥如 君（D01B48013 ）在國立臺灣大學 基因體與系統生物學學位學程完成之博士學位論文，於民國 109 年 3 月 19 日承下列考試委員審查通過及口試及格，特此證明。

口試委員：

（簽名）

（指導教授）

學程主任 （簽章）

doi:10.6342/NTU202000765

致謝

在寫下誌謝的同時，代表博士班的時光即將畫下句點，這麼多年的時間就在不知不覺中飛逝。回首這幾年的研究時光多是平靜且踏實的，並不像許多人在博班過程中經歷後悔掙扎，因為我總認為當下定決心後就沒有什麼好後悔猶豫的，當目標堅定就能一步步走過這條漫長的道路。在完成論文後也體會到，學習過程中有太多無形的收穫比實質的學位更可貴。而一個讓自己變得更好的過程中，需要感謝的是身邊支持著你，讓你有足夠能量堅持到底的每個人。

最要感謝的是莊樹諄老師，在博士班期間給予我充分的指導與支援。在科學的領域中當我還在看著小河流的時候，老師帶著我經過一次次的討論，逐步調整研究方向並擬定新的研究策略，最後帶我看見大海。他嚴謹細緻的科學態度和按部就班的工作風格，都將成為我學習的榜樣。此外，也感謝研究過程中給予我協助和建議的每一位口試委員及教授。

這段期間, 讓我覺得最幸運的是實驗室的同仁們都如同小天使般幫助著我。在這個大數據分析實驗室，要學習的領域有很多，如果單靠我一個人的力量是沒有辦法完成這篇論文的。其中尤其感謝嘉瑩、德倫和泰緯，他們在統計和程式撰寫上給予我很多協助和指導，幫助我一步步克服研究上的難關，在此深表感謝。

最後想要感謝我的家人，一直以來對我所做的決定都給予支持與鼓勵。因為你們我才能完成自己的理想和目標，因為你們我才能成為今天的我。小時候想當一個科學家，覺得科學家很厲害，能發現很多驚奇的事物。長大後發現，原來想當個真正的科學家並不是這麼容易啊。但如今完成了這個博士學位, 也算是圓了小時候的一個心願吧。

doi:10.6342/NTU202000765

中文摘要

自閉症譜系障礙是一種腦部發展障礙所導致的複雜疾病，患者特徵有社交溝通與互動障礙，侷限且重複的行為或興趣，有些伴隨不同程度語言發展障礙。在已開發國家中約有 1-2% 孩童被診斷罹患自閉症。普遍認為自閉症與遺傳因素有相當大的關係，然而患者間在基因變異上有很大的差異，因此目前對自閉症的致病機轉仍不甚了解。許多研究發現自閉症與特定的基因變異有關，其所影響的功能多和神經元活性及可塑性、突觸連結以及免疫和發炎反應等相關。而在核糖核酸[1]層次上，後轉錄調控機制是否參與在自閉症致病機轉仍不甚了解，尚待進一步探討。

藉由人腦組織的轉錄體與表觀基因體分析發現，許多自閉症患者上表現異常的生物標記，如信使 RNA （mRNA）、 微小 RNA （miRNA） 、長非編碼 RNA （lncRNA）、多樣性切割以及各種表觀遺傳因子等。近年來陸續有研究指出，環狀 RNA（circRNA）與許多神經疾病的發生與神經發育有關，因此具有重要研究價值。環狀 RNA 是一種非線性 RNA，經由先導 mRNA 反式剪接而成，具有共價閉合的單鏈環狀結構。circRNA 能扮演一種 miRNA 海綿效應，結合互補的 miRNA，使其無法抑制下游基因轉錄，而這樣的機轉也被報導在許多神經疾病中，但 circRNA 是否參與在自閉症調控機轉中目前尚未被探討。

本篇研究中，我們整合上百筆人腦組織的轉錄體定序數據，揭開自閉症患者和非自閉症大腦中 circRNA 的表現圖譜，發現自閉症患者大腦皮質中存在六十個表現量異常的環狀 RNA 以及三群共同表達的 circRNA。經由整合 mRNA、miRNA 和 circRNA 表現量資料，以及預測 miRNA 結合為結合位，建立出自閉症相關的 circRNA–miRNA–基因調控網路。最後我們證實一個在自閉症患者腦部表現量明顯上升的環狀 RNA（circARID1A），它能吸附 miR-204-3p 進而影響多個自閉症相關基因的表達。這顯示自閉症除了受到風險基因突變影響外，也可能藉 circRNA 調控 miRNA，進而影響下游基因表達。而 circRNA–miRNA–基因調控網路的預測方法，未來也可應用在其他複雜神經疾病中，為複雜疾病診斷、追蹤及治療提供新的思考方向。

doi:10.6342/NTU202000765

關鍵字：自閉症、環狀核糖核酸、微小核糖核酸、基因調控網路

doi:10.6342/NTU202000765

Abstract

Autism spectrum disorders (ASDs) are a heterogeneous group of complex neurodevelopmental disorders characterized by impairment in social, communication, and restricted or repetitive behaviors. Despite remarkable genetic heterogeneity, ASD-associated genes have been suggested to target a few convergent biological processes, including synaptic transmission and plasticity, neural activity, and metabolism-related. However, the role of post-transcriptional mechanisms in ASD is largely uncharacterized.

In recent years, through analysis of transcriptome and epitranscriptome of human brain tissues, many biomarkers such as messenger RNA (mRNA), microRNA (miRNA), long non-coding RNA, alternatively spliced transcript and various epigenetic factors have been found in ASD patients. Several studies have suggested that circRNAs are involved in the occurrence and development of neurological diseases. Currently, much less is known about the contribution of circRNA in regulatory mechanisms of ASD. Circular RNA (circRNA) is a type of endogenous non-co-linear RNA, which are covalently closed single-stranded RNA molecules derived from the backsplicing of pre-mRNAs. CircRNAs play a regulatory role as miRNA sponges to suppress the downstream targets of complementary miRNAs.

In this study, we performed genome-wide circRNAs expression profiling in post-mortem brains from ASD and non-ASD samples. Our analysis revealed 60 differential expressed circRNAs and three perturbed co-regulated modules in ASD. We explored ASD-associated circRNA–miRNA–mRNA interactions, in which target genes were

doi:10.6342/NTU202000765

particularly enriched for ASD risk genes and genes encoding inhibitory postsynaptic density proteins. Furthermore, we confirmed that some ASD risk genes were indeed regulated by circARID1A via sponging miR-204-3p in human neuronal cells. Our genome-wide analysis provides a deeper insight into the role of dysregulated circRNAs, as well as the corresponding circRNA–miRNA–mRNA axes in ASD pathophysiology.

Keywords：Autism spectrum disorder, ASD, circular RNA, circRNA-microRNA-mRNA, circARID1A, has-miR-204-3p

doi:10.6342/NTU202000765

Table of contents

doi:10.6342/NTU202000765

doi:10.6342/NTU202000765

List of Figures

doi:10.6342/NTU202000765

doi:10.6342/NTU202000765

List of Tables

doi:10.6342/NTU202000765

CHAPTER 1. Introduction

1.1 Autism spectrum disorder (ASD)

1.1.1 Overview of ASD

ASD is the most common neurodevelopmental disorders observed in childhood, which is a group of complex neurodevelopment disorders. ASD is defined by a deficit in social communication and interaction, restricted interests and repetitive behaviors[2-4] (Fig. 1A). In the new systems, language ability is not a core diagnostic criterion of ASD, because level of language skill is highly variable in ASD. The worldwide prevalence of autism is about 1-2%, which has continued to rise in the past decades[5-7].

The two new diagnostic systems for autism characteristics are the Diagnostic and Statistical Manual of Mental Disorders (DSM-5), fifth edition, which was compiled by the American Psychiatric Association (APA), and the 11th revision of the International Classification of Diseases (ICD-11), which was published by the World Health Organization (WHO). Autism is known as a "spectrum" diagnosis because there is wide variation in the severities and abilities (IQ, language, etc), which can be subgrouped into autistic disorder, Asperger syndrome, pervasive developmental disorder not otherwise specified (PDD-NOS), and childhood disintegrative disorder (CDD)[8] (Fig. 1B).

Autism was categorized as syndromic or non-syndromic. Most cases of ASD are non-syndromic which influenced by the small effects of many genes. A small part of ASD co-occurring with clinically defined genetic syndromes, such as Fragile X syndrome

doi:10.6342/NTU202000765

(FXS), Rett's disorder (RTT), MECP2 duplication syndrome (MDS) and Tuberous sclerosis were classified as syndromic ASD[9].

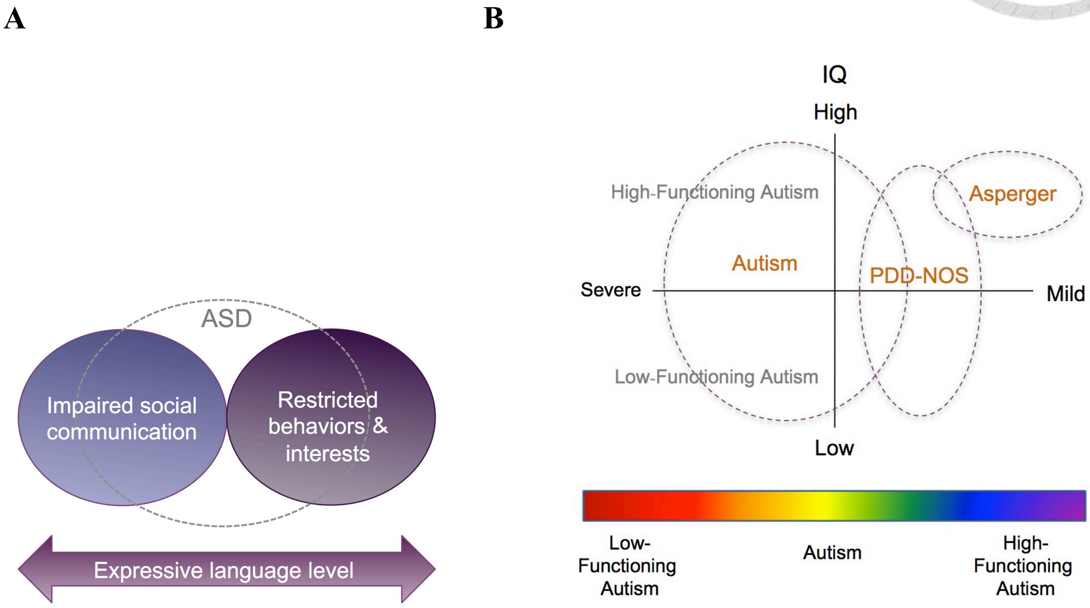

Figure 1. (A) DSM-5 classification system for ASD. (B) Classification of ASD based on severity and intellectual development.

(A) The definition of ASD by DSM-5. The figure is adapted from[10]. (B) The relationship between degree of atypicality severity and IQ of ASD.

1.1.2 Neurobiology and co-occurring conditions of ASD

Functional magnetic resonance imaging (fMRI) studies have revealed that children with ASD have increased volume of brain and amygdala and reduced volume of corpus callosum[11]. The post-mortem studies observed that the neuron number in the amygdala, fusiform gyrus and cerebellum were reduced[12,13]. However, the neuron number in the prefrontal cortex was increased[14]. In addition, frontal lobes, temporal lobes and cerebellar vermis have been reported to be the main regions implicated in dysfunction in autism[15,16]. The medial prefrontal cortex, superior temporal sulcus, temporoparietal junction, amygdala, and fusiform gyrus are hypo-active in autism[17-19]. Several lines of

doi:10.6342/NTU202000765

evidence implied that autism is characterised by abnormal brain connectivity[20]. The brain of autism often reduced global connectivity and increased local connectivity[21], decreased frontal-posterior cortical connectivity, and enhanced parietal-occipital connectivity[22,23]. Local information processing involves sensory and perceptual inputs; global information processing integrates higher-level cortical control, which is important in social interaction and communication[24].

Additionally, more than 70% of people with ASD tend to co-occur with ASD-associated concurrent developmental, medical and psychiatric conditions[24,25]. The detailed information was listed in Table 1.

Table 1. Common concurrent clinical disorders in ASD.

	Conditions	Proportion*	Reference
Developmental	Intellectual disability	30-40%	26
	Sensory processing dysfunction	70-96%	27,28
	Attention-deficit hyperactivity disorder	28.2% 25.7%	29 30
	Language disorders	Variable	
Medical	Epilepsy	20%	31
	Gastrointestinal disorder	23-70%	32
	Immune dysregulation	46%	33
	Sleep disorder	60-86%	34
Psychiatric	Anxiety	42-79% 27-42%	35 36
	Depression	23-37%	36
	Psychotic disorders	54.8%	30

* Proportion of individuals with ASD present co-occurring conditions.

1.1.3 The heritability and genetic basis of Autism

Many causes are reported to be implicated in ASD, including genetic (e.g., rare, common or de novo mutated[37,38] and copy number variations[39,40]) and non-genetic (e.g.,

doi:10.6342/NTU202000765

environment[3,41], parental reproductive age[42,43], and gestational factors[44,45]) factors. Although the exact mechanism of ASD still remains unknown, the weight of evidence suggests that genetic factors may be the major cause for autism spectrum disorders.

Twin studies have suggested that autism has approximately 80% heritability[46,47]. The concordance rates of ASD for monozygotic twins (50–90%) are much higher than dizygotic twins (0–36%)[47-50], again indicating strong genetic influences on ASD. On the other hand, the recurrence rate of ASD in families who already have one affected sibling, with recurrence estimates ranging from 5.8% to 18.7%[51-53].

Over the past decade, several studies showed that thousands of genes and thousands of rare variants were associated with ASD susceptibility[48,54,55]. Several strongly ASD-associated genes have been identified, including postsynaptic scaffolding genes (*SHANK3*)[56], synaptic plasticity (*SYNGAP1*)[57], and neurexin family genes (*CNTNAP2*)[58]. Besides, some of individuals with ASD were found to be linked to chromosomal rearrangements or single gene disorder, such as fragile X syndrome[59] (CGG trinucleotide repeat expansion in the *FMR1* promoter) and Rett syndrome[60] (mutations that inactivate *MECP2*). Recently, many genome-wide studies have reported ASD-associated dysregulation of gene expression[15,16,61] and epigenetic factors such as alternatively spliced transcripts[15,16,62], long non-coding RNAs[16,63], miRNAs[64,65], DNA methylation[66], histone trimethylation[67], acetylation[68] and so on. The contribution of these genetic factors to this complex disease is highly heterogeneous. Despite remarkable genetic heterogeneity, ASD-associated genes have been suggested to target

doi:10.6342/NTU202000765

convergent biological pathways[69], such as synaptic function[15,70,71], transcriptional regulation[71], neural cell adhesion[72,73], immune/inflammatory responses[74,75] and excitatory/inhibitory (E/I) neuronal balance[76,77].

Several studies in small population have explored gene expression profiles in ASD brain regions[78-81]. Most of the genes surveyed were exposed to be consistently up- or down-regulated in different studies[82]. This strongly implies that these genes are not coincidentally up- or down- regulated, but might actually have roles in the underlying pathogenesis of ASD. Recently, Daniel H. Geschwind's group performed large-scale of genome-wide mRNA[16] and miRNA[64] expression profiling of post-mortem brains in ASD. Now, integration and dissection of the role of co-/post-transcriptional regulatory mechanisms in the etiology of ASD await further investigation.

1.2 Circular RNA (circRNA)

1.2.1 Characteristics of circRNAs

CircRNAs are a large class of non-coding RNAs produced by thousands of protein-coding genes, which are circularized by non-canonical "backsplicing" of pre-mRNAs[83,84]. CircRNAs are single-strand circular molecules without 5' cap or 3' poly(A) tail (Fig. 2). Owing to this structure, circRNAs are resistant to degradation by exonucleases RNase R[85-87] and relatively stable than their corresponding co-linear mRNA isoforms[86-89]. In 1970s, circRNAs were firstly discovered in RNA viruses by electron microscopy[90] and later in eukaryotic cells in 1979[91]. Until 1991, circRNAs were firstly identified in human[92]. In the beginning, circRNAs were thought as by-

doi:10.6342/NTU202000765

product of pre-RNA splicing. These recent years, increasing evidence shows the roles of circRNAs in the development and diseases.

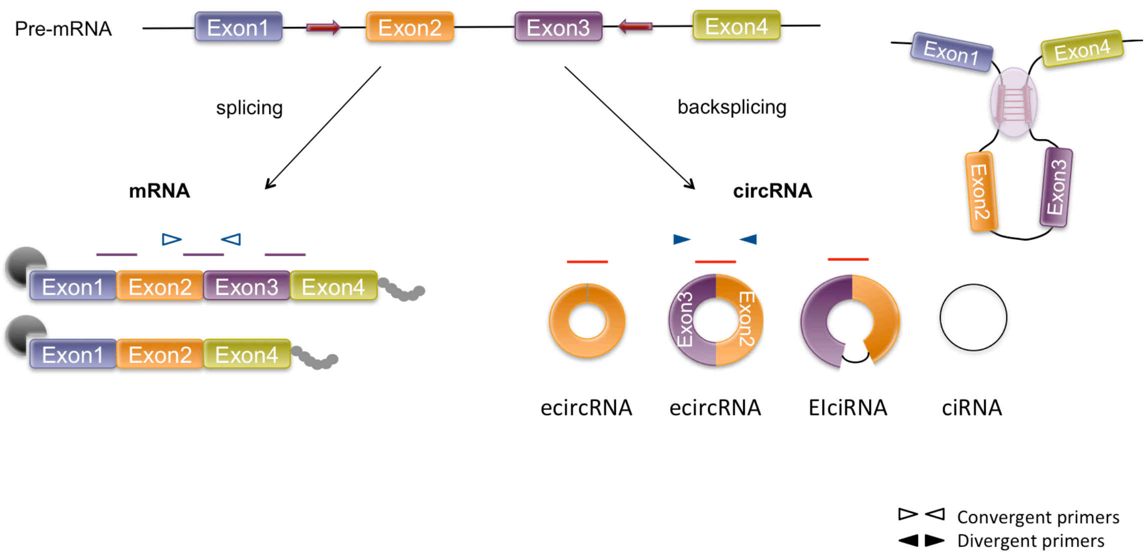

Figure 2. Schematic representation of the biogenesis of circRNAs.

1.2.2 Biogenesis of circRNAs

According to biogenesis from different genomic regions, circRNAs can be classified into three subtypes: exonic circular RNAs (ecircRNAs), exon-intron circular RNAs (EIciRNAs), and circular intronic RNAs (ciRNAs) (Fig. 2). More than 80% of circRNAs are derived from exons of protein-coding genes without introns, constituting ecircRNAs[86]. Approximately 20% of circRNAs are derived from both exonic and intronic regions, constituting exon-intron circular RNAs (EIciRNAs)[93]. A small fraction of circRNAs contain only introns regions, termed circular intronic RNAs (ciRNAs), which stem from spliced out lariats[94].

CircRNAs formation can be modulated by *cis*-elements, *trans*-factors and other factors.

doi:10.6342/NTU202000765

1) *Cis*-elements (i.e., DNA sequences):

CircRNA biogenesis can be promoted by RNA pairing between the reversely complementary sequences (RCSs) across flanking introns[87,95] (Fig. 2). Further studies indicated that the flanking introns of circRNA junctions were longer than background introns and harbored more repetitive elements[87,96]. Our previous study has demonstrated that RCSs (*Alu* repeats) across flanking introns can affect the formation of both circRNA and *trans*-spliced RNA isoforms[89]. Nevertheless, no specific motifs for circRNA formation have been identified in exonic and flanking intron sequences.

2) *Trans*-factors (i.e., RNA binding proteins, RBPs):

In addition to *cis*-element, circRNAs can also be facilitated by *trans*-factors to bridge flanking introns pairing[97,98]. Some splicing factors (e.g. Muscleblind (MBL)[83], Quaking (QKI)[97]) and RNA-binding proteins (e.g. FUS[99], ADAR[100]) can affect circRNA formation. MBL was shown to bind to its own pre-mRNA and bridging between the two flanking introns to induce backsplicing, which stimulates circMbl production and decrease the expression level of MBL mRNA[83]. Another regulator of circRNA biogenesis is QKI which binding on intronic QKI binding motifs, then significantly increased circRNA formation[97]. FUS promote backsplicing by binding the flanking introns of circularized exons[99]. Conversely, ADAR1 protein suppresses circRNA formation by disrupting the stem structure. ADARs catalyze A-to-I RNA editing within double stranded RNA pairing structures, resulting in reduced RNA pairing[100].

3) Spliceosome activity and Pol II elongation rate:

A recent study has found that depletion of spliceosome activity increased long and repeat-rich flanking intron[101] and non-complementary sequences[102] to pair, facilitating

doi:10.6342/NTU202000765

circRNA formation. Besides, the process of circRNA formation was also influenced by the transcription rate of the corresponding gene. The average Pol II transcription elongation rate of circRNA host genes is higher than that of non-circRNA genes[84].

1.2.3 Expression of circRNAs

CircRNAs exhibit evolutionary conservation across multiple species, and exists widely in eukaryotes[87]. Several studies reported that circRNAs are enriched in neuronal tissues compared with other tissues[103-105], especially synaptosomes[105]. That prompting many researchers to explore the role of circRNAs in neurological diseases. Most of circRNAs are enriched in the cytoplasm[85,106], suggesting that circRNAs regulate gene expression through interfering with miRNAs. In general, circRNAs are expressed in a tissue- or age-dependent manner[107,108], and also show dynamic expression during neuronal differentiation, depolarization and development[104,109,110].

Multiple studies have demonstrated that the expression of circular isoform was not correlated with the expression of its cognate linear mRNA[103]. Although most circRNAs are expressed at a much lower level compared with their host gene[81,111,112]. However, in some cases, circRNAs even more abundant than their co-linear counterparts[88,89]. For example, Morten, et al. found that the expression of three circRNA (circCSPP1, circHDAC2, and circRIMS2) were much higher than those of the linear transcript in porcine brain, and their host gene were associated with synaptic plasticity or brain development[104].

doi:10.6342/NTU202000765

1.2.4 Regulation of circRNAs

Although the function of circRNAs is not entirely clear, the recent studies have shown that circRNAs may have the ability to regulate gene expression through multiple mechanisms[106] (Table 2). The most understood function of circRNAs is the regulatory role of miRNA sponges, suggesting a previously underappreciated regulatory pathway of circRNA-miRNA-mRNA axes. For example, CDR1as is one of the most widely studied circRNA, which has more than 70 binding sites for miR-7 and function as an miRNA sponge to compete with mRNA for miRNA binding[113]. In addition, certain circRNAs can regulate transcription. For example, circMbl negatively regulate MBL pre-mRNA splicing by competing the splicing factors[83]. EIciRNAs are dominantly located in the nucleus and interact with a spliceosomal component U1 snRNPs, which can recruit RNA polymerase II on the promoter of their host genes and thus promote the transcription of the host gene, such as EIciEIF3J, EIciPAIP2 and Ci-ankrd52[93,94]. Another study demonstrated that circERBB2 can promotes ribosomal DNA transcription[114]. In contrast, circSamd4 can represses transcription of the myosin heavy chain protein family by associated with PURA and PURB, two repressors of myogenesis[115].

On the other hand, many circRNAs interact with proteins through specific binding sites[116]. In their function as protein decoys, circPABPN1 serve as a decoy for HuR and suppresses PABPN1 translation[117]. Besides, circ-Amotl1 bind to c-Myc, promoting their nuclear translocation, and upregulated its targets[118]. Additionally, circANRIL has similar secondary structure to pre-rRNA, which decoys PES1 to suppress rRNA

doi:10.6342/NTU202000765

processing and maturation[119]. CircRNAs can also function as scaffolds to facilitate subcellular co-localization of their substrates. Circ-Foxo3 acts as scaffold to interact with CDK2 and p21, and then leading to the inhibition of the CDK function[120]. Circ-Foxo3 also promotes the interaction between MDM2 and p53 to induces apoptosis[121]. Specifically, circ-Foxo3 affected ID1, E2F1, HIF1α and FAK subcellular translocation[122]; circ-Amotl1 interacts with PDK1 and AKT1 to facilitate their nuclear translocation[123]. Moreover, some protein-coding circRNAs contain internal ribosome entry site (IRES) and open reading frame, such as circ-ZNF609[124], circ-FBXW7[125], circ-AKT3[126] and circPPP1R12A[127] can be translated to produce peptides (Table 2).

One of the most well-known functions of circRNAs is the role of miRNA sponge to regulate target gene expression[113]. Several data indicated that the interactions between circRNAs and miRNAs were important for normal brain function. For example, CDR1as knockdown mice displays impaired sensorimotor gating and abnormal synaptic transmission[128]. Therefore, it is believed that circRNAs can mediate miRNAs and thus regulate the downstream genes at the post-transcriptional level. While some cases of ASD-associated miRNA–mRNA regulatory interactions have been reported[64,129], circRNA–miRNA–mRNA regulatory system may play an important mechanism of epigenetic control over gene expression in ASD and healthy samples.

doi:10.6342/NTU202000765

Table 2. Potential functions of circRNAs.

Function	circRNAs	References
miRNA sponge	CDR1as / Sry / circHIPK3/ circMTO1 / circITCH / circCCDC66 / circTP63	86,88,113,130-133
Regulation of transcription	circMbl / EIciEIF3J / EIciPAIP2 / Ci-ankrd52 / circERBB2 / circSamd4	83,93,94,114,115
Protein decoys	circPABPN1 / circ-Amotl1 / circANRIL	117-119
Protein scaffolds	circ-Foxo3 / circ-Amotl1	120-123
Translation peptides	circ-ZNF609 / circ-FBXW7 / circ-AKT3 / circPPP1R12A	124-127

1.2.5 CircRNAs in neurological diseases

CircRNAs expressed in fly heads or mouse brains are enriched in genes that code for neuronal proteins and synaptic factors, suggesting a potential role for circRNA in the central nervous system[105,107]. Moreover, several cases of circRNAs show distinct localization in different parts of neurons[103], their host genes are related to several synaptic functions, including neurogenesis, neural differentiation, WNT signaling, and synaptic plasticity during neurogenesis[103-105]. Therefore, circRNAs have the potential to serve as novel therapeutic targets and diagnosis biomarkers to treat neurological diseases, such as Alzheimer's disease[134], Parkinson’s disease[135], major depressive disorder[136], and many nervous system disorders[137] (Table 3).

These studies highlight a potential function of circRNAs in the nervous systems and suggest their relevance to pathogenesis of neurodegenerative. However, the biological functions of circRNA regulatory mechanisms in ASD are largely unknown.

doi:10.6342/NTU202000765

Table 3. Representative circRNAs and related regulatory interactions in neurological diseases.

Neurological diseases	circRNAs	Intersection molecules*	References
Alzheimer's disease	CDR1as	→miR-7 →UBE2A →APP & BACE1	134 138 139
Parkinson's disease	CDR1as	→miR-7 →SNCA	113
Major depressive disorder	circRNA_103636		136
Neuropathic pain	rno_circ_0006298	→miR-184	140
Multiple system atrophy	IQCK, MAP4K3, EFCAB11, DTNA, MCTP1		141
Neurological Tumors	circ-FBXW7	→FBXW7-185aa	125 142
Neuroinflammatory	circHIPK2	→miR124 →SIGMAR1/OPRS1	143
Dysfunction of excitatory synaptic transmission	CDR1as	→miR-7 & miR-671 →Fos	128
Neurotoxicity	circRar1	→miR-671 →caspase-8 & p38 pathway	144
Cerebral ischemia-reperfusion injury (IRI)	mmu-circ-015947 mmu_circRNA_40001, mmu_circRNA_013120, mmu_circRNA_40806		145 146
Ischemic stroke	circDLGP4 circHECTD1	→miR-143 →miR-142	147 148

* Intersection molecules represent the downstream pathway of circRNAs.

1.3 Detection and validation of circRNAs

1.3.1 Detection of circRNAs by bioinformatics and statistical methods

CircRNAs can be detected from RNA sequencing (RNA-seq) and microarray using computational approaches to identify the back-spliced junction (BSJ). Total RNA-seq with ribosomal RNA (rRNA) depletion or RNase R treatment are most commonly used for circRNA profiling[149]. Usage of paired-end reads for identifying circRNAs could help us to filter out false positive circRNAs, if the paired-end of a read out of the predicted circles[150].

doi:10.6342/NTU202000765

Currently, numerous circRNA detection tools (circRNA_finder, CIRCexplorer, find_circ, etc.) have been developed. However, there are great inconsistencies in the results among different tools[151]. A recent article compared the performance of several published algorithms, finding dramatic differences between sensitivity and specificity[152]. Notable, NCLScan[153] was a conservative method with the highest precision compared with currently circRNA detectors[154]. It constructs the putative non-co-linear (NCL) references from the unmapped paired-end reads and BLAT-aligning the concatenated sequences to the reference genome. Then, removing concatenated sequences with an alternative co-linear explanation[153]. The pipeline carries out several alignments and filtering and integrates with BWA, Novoalign and BLAT to reduce false positives. Accordingly, we identified circRNAs by the NCLscan (version 1.6) to detect BSJ reads from RNA-seq data.

1.3.2 Validation of circRNAs by experimental methods

CircRNAs can be validated by some experimental methods. First, the most basic approach is to detect the BSJ reads by divergent primer PCR (Fig. 2). However, *trans*-splicing transcripts[155] (splicing between two separate pre-mRNA) and template switching[156] can lead to false positive events of circRNA. Therefore, researcher can use MMLV- and AMV- derived RTases to exclude template switching by reverse transcription (RT)[157], and use exoribonuclease RNase R to degrade linear form of *trans*-splicing transcripts[158]. Sanger sequencing can validate the BSJ sequence, and the expression level of circRNAs can be quantified by quantitative real-time PCR.

doi:10.6342/NTU202000765

Moreover, if circular and linear RNA exhibit different sizes, circRNA can be confirmed by northern blots and fluorescence in situ hybridization [37,159]. The procedures of northern blots and FISH do not involve RT or PCR amplification that can avoid detecting false positives from RT-based artifacts. However, it can only detect highly expressed candidates.

For functional study, circRNAs overexpression and knockdown are two typical ways. For mechanism study, luciferase reporter assay, RNA pull down assay, RNA immunoprecipitation, and mass spectrometry are performed to uncover circRNA interactions[106].

1.4 Purpose of this study

To systematically determine regulatory role of circRNAs in ASD, we investigated the expression profile and potential regulatory role of circRNAs in ASD. Our study aimed to integrate the expression of circRNA, miRNA and mRNA to investigate circRNA dysregulation in ASD, and construct the ASD-associated circRNA–miRNA–mRNA regulatory networks according to the common target miRNAs of the circRNAs and mRNAs. That may open a new approach to take a global view of heterogeneous diseases, and unveil the potential mechanisms of circRNAs and may lead to improve ASD diagnosis and treatment in the future.

doi:10.6342/NTU202000765

CHAPTER 2. Materials and methods

2.1 Identification and quantification of circRNAs in human brain

We collected the rRNA-depleted total RNA-seq data from Synapse (https://www.synapse.org) under accession number syn4587609. A total of 236 post-mortem samples included frontal cortex (FC, Brodmann area 9), temporal cortex (TC, Brodmann area 22, 41 and 42), and cerebellar vermis (CV) from 48 individuals with ASD and 49 non-ASD controls (CTL)[16].

For circRNA quantification, we used some criteria to improve accuracy. Fist, the samples were not considered in the following analysis if the number of the identified circRNAs of these samples were one standard deviation below the mean. Therefore, 202 samples (73 FC, 61 TC, and 68 CV samples) were retained. Second, since several studies of ASD have illustrated that human cortex has been implicated in the pathophysiology of ASD[160,161], and changes in transcriptome were more evident in the cortex than in the cerebellum[16]. Accordingly, our following analysis focused on frontal and temporal cortex. Third, to reduce potentially spurious events, we only considered the circRNAs that were expressed (≥ 10 reads) in more than 50% of the 134 cortex samples. Thus, a total of 1,060 circRNAs were used in the following analyses.

CircRNAs were identified by NCLscan program which was reported to exhibit the greatest precision among currently circRNA-detection tools[153,154,162,163]. To align the reads to the human reference genome (GRCh38, Ensembl 90) with default parameters.

doi:10.6342/NTU202000765

The previously identified human and mouse circRNAs were obtained from circBase[164] and CIRCpedia[165] version 2 database. Since circBase use the hg19 assembly for human circRNA, so we converted the genomic coordinates of circRNAs from hg19 to GRCh38 assembly using the liftOver tool[166]. Also, the coordinates of mouse circRNAs collected in circBase (mm9) and CIRCpedia (mm10) were transformed to the corresponding GRCh38 coordinates by the liftOver[166].

2.2 Identification of differentially expressed circRNAs (DE-circRNAs)

For estimated of circRNA abundance in different dataset, the total number of BSJ-spanning reads per million uniquely mapped reads (RPM) was used for measuring circRNA expression level[104]. Therefore, RPM = number of junction reads / (number of mapped reads/10^6). The read counts of the host genes were calculated by the STAR aligner[167], followed by the RSEM tool. The expression level of genes were measured by $\log_2$ normalized FPKM (normalized GC content, gene length, and library size) using the cqn package in R[168].

Many methods have been proposed to identify differentially expressed expression. The expression of circRNA is potentially affected by many confounding factors. Here we used the 'nlme' package in R[169] to control potential confounding factors, including sex, age, brain region (FC or TC), RNA quality (RNA integrity number; RIN), post-mortem interval (PMI), host gene expression, sequencing batch, and brain bank batch. We performed LME model to identified DE-circRNAs between ASD and non-ASD samples with controlling for potential confounding factors:

doi:10.6342/NTU202000765

lme (RPM~ diagnosis + sex + age + brain region + RIN + host gene expression + sequencing batch + brain bank batch, rand = ~1|individual ID)

The model can fix different factors to estimate *p* values for each circRNAs. *P*-values < 0.05 and | log2 (fold change) | > 0.5 were considered evidence of significant difference.

2.3 Weighted gene co-expression network analysis (WGCNA) analysis

Gene co-expression network was constructed by the R package WGCNA[170] to identify co-expression modules in this study. It is a data mining method for studying biological networks with pairwise correlations between variables, and to identify groups of highly correlated genes that co-express across samples. We present the Dynamic Tree Cut R library with function cutreeDynamic, in which the paramenters are: method = "hybrid", deepSplit = 3, pamStage = T, pamRespectsDendro = T, minClusterSize = 10, for detecting clusters in a dendrogram depending on their shape. The expression of each module was summarized by the eigengene (ME), which can be considered as the first principal component of a given module. To identify diagnosis status, the Pearson Coefficient between circRNAs and several confounding factors (diagnosis, age, sex, brain region, RIN) were calculated. All circRNA–miRNA–mRNA networks were visualized by Cytoscape software[171] (https://cytoscape.org/).

2.4 MicroRNA binding sites prediction

In summary, we identified 60 DE-circRNAs (22 upregulated and 38 downregulated circRNAs) and three DE-modules (one upregulated module included 21 circRNAs and two downregulated modules included 298 circRNAs) in ASD cortex. In order to

doi:10.6342/NTU202000765

identified ASD-associated circRNA–miRNA–mRNA regulatory axes. We collected previous study which have evaluated 58 DE-miRNAs (41 upregulated and 17 downregulated miRNAs) in ASD cortex[64]. These ASD-affected miRNAs were identified from 95 human cortex samples (47 ASD and 48 non-ASD samples), of which 73 samples overlapped with the samples examined in this study.

To investigate the interaction between dysregulated circRNA and miRNA, we used RNA22[172] (version 2.0) with default parameters to predict 58 miRNA binding sites on 60 DE-circRNAs and the circRNAs defined in the DE-modules (Fig.3). RNA22 allows identifying putative target sites of novel miRNAs on any sequence of interest (i.e. protein-coding mRNA, long non-coding RNA or non-canonical targets). Thus, a total of 808 potential circRNA–miRNA interactions were identified.

Next, to investigate putative target mRNA of 58 dysregulated miRNA, we combine the miRNA–mRNA pairs from multiple sources. For 37 well annotated miRNAs, we identified downstream targets by the microRNA Target Filter in Ingenuity Pathway Analysis package[173,174] (QIAGEN Inc.) and DIANA-TarBase v8[175]. The IPA provides experimentally validated interactions collected by Ingenuity Expert Findings, as well as predicted microRNA-mRNA interactions by TargetScan[176]. TarBase collected experimentally confirmed miRNA targets (Fig.3). To obtain reliable interactions, the miRNA–mRNA binding events were considered if one of the following three criteria is satisfied:

doi:10.6342/NTU202000765

1) TargetScan predicted interaction with context++ score < -0.16, and also identified by Wu et al.[64].

2) Experimentally confirmed events collected by Ingenuity Expert Findings, which were manually curated by the IPA experts.

3) Experimentally confirmed events collected in TarBase.

For the other 21 novel miRNAs, we use miRDB[177,178] to predicted downstream targets with prediction scores > 80. The mature miRNA sequences were downloaded from the study of Wu et al[64]. For accuracy, we only considered the predicted miRNA–mRNA interactions that were also previously identified by Wu et al.[64]. Thus, a total of 36,512 miRNA–mRNA interactions were determined (Fig.3).

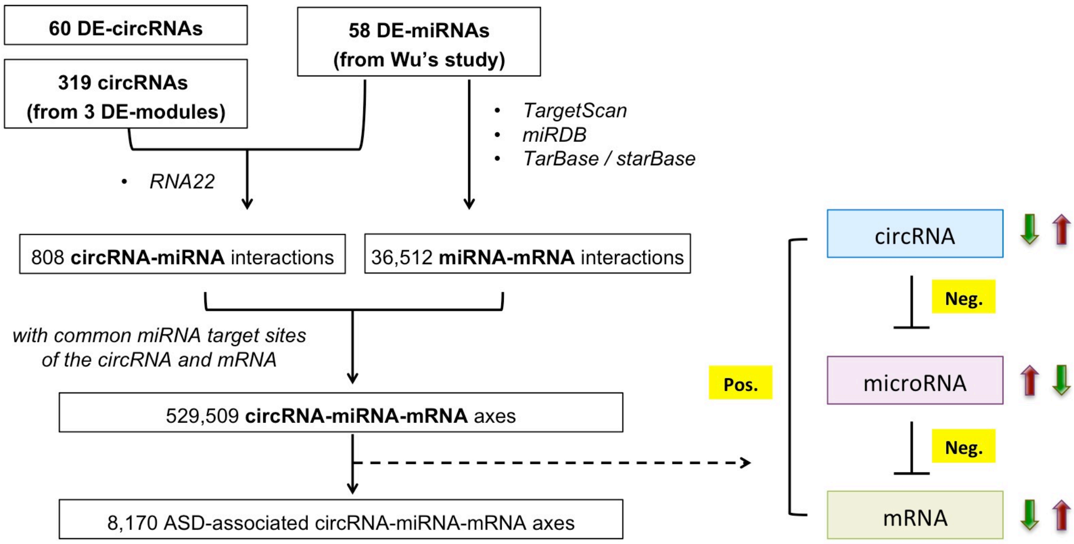

Figure 3. Identification processes of the potential ASD-associated circRNA-miRNA-mRNA axes.

"Neg." represents a negative correlation; "Pos." represents a positive correlation. The red arrow represents upregulation; the green arrow represents downregulation.

doi:10.6342/NTU202000765

2.5 Construction of ASD-associated circRNA–miRNA–mRNA networks

The expression level of the target genes were measured by $\log_2$ normalized FPKM, which accounted for gene read counts, GC content, gene length, and library size, using the cqn program in the R package. The miRNAs expression data was obtained from Prof. Daniel H. Geschwind and Ye E. Wu[64], which was measured by normalized read counts with controlling library size, GC content, batch effect, and other technical covariates (RIN, PMI, and batch bank).

We integrated the identified interactions for 808 circRNA–miRNA interactions and 36,512 miRNA–mRNA interactions; we determined 529,509 circRNA–miRNA–mRNA interactions according to the common miRNA target sites of the circRNAs and mRNAs (Fig.3). We then calculated the correlations between circRNA and miRNA expression, between miRNA and mRNA expression, and between circRNA and mRNA expression based on the same set of cortex samples (i.e., 73 samples). Only the circRNA–miRNA–mRNA interactions were considered if they simultaneously satisfied the following rules:

1) Both the circRNA–miRNA and miRNA–mRNA pairs should exhibit a significantly negative correlation (one-tailed Spearman's $P < 0.05$) of expression profile, between circRNAs and the corresponding predicted regulated miRNAs and between miRNAs and target mRNAs, respectively.
2) The circRNA expression should be positively correlated with the corresponding mRNA expression.
3) The Fisher's combined P values[179] of the above three independent Spearman's correlation tests should be less than 0.05.

doi:10.6342/NTU202000765

Finally, 8,170 ASD-associated circRNA–miRNA–mRNA regulatory axes were determined, which included 2,302 target genes (Fig.3).

2.6 Gene set enrichment analysis

The SFARI[180] gene list was downloaded from https://gene.sfari.org/. The high-confidence ASD genetic risk genes (102 genes)[181] were derived from an enhanced Bayesian analytic framework based on a large dataset of whole-exome sequencing (35,584 ASD subjects). The epilepsy-related gene list was downloaded from the EpilepsyGene database[182] (all epilepsy-related genes). The schizophrenia-related gene lists was downloaded from the SZgene database[183]. The genes associated with human height were downloaded from the study of Lango Allen et al.[184]. The gene lists of AustismKB, iPSD, ePSD, and other brain disorder risk genes were downloaded from the study of Wang, P., et al.[185] Gene set enrichment analysis were performed using two-tailed Fisher's exact test with the fisher.test R function. Phenotype ontology analysis was performed by the ToppFun module of ToppGene Suite software[186]. *P* values were false discovery rate (FDR) adjusted across 14 target groups for each gene list using Bonferroni correction.

2.7 Cell culture

To study the function of circRNAs for neural cells interact, we relies on the use of human neural progenitor (ReNcell VM) cell[187,188], primary normal human astrocytes cell (NHA), human glioblastoma cell (U118) and human neuroblastoma cell (SH-SY5Y). ReNcell is a valuable material for investigating neurodevelopmental

doi:10.6342/NTU202000765

pathway[189], which provided by Prof. Jean Lu. The ReNCell was grown on 20 μg/ml laminin (Merck) coated culture plates containing ReNCell NSC maintenance medium (Merck) supplemented with 20 ng/ml of bFGF and EGF (Merck). NHA cell line was purchased from Gibco (N7805100) and cultured in Human Astrocytes Growth medium (Cell Applications). U118 cell line was purchased from ATCC (HTB-15) maintained in Dulbecco's modified Eagle's medium. SH-SY5Y cell line was obtained from ATCC (CRL-2266) and cultured in DMEM/F12 medium (Gibco). All culture media contain 10% fetal bovine serum (FBS) and 5 mg/ml antibiotic-antimycotic (Gibco), and growth at 37% and 5% CO2. Cells were passaged when the confluence reached 80% of the culture plate every three to four days. Briefly, cells were rinsed with PBS and then incubated in Accutase (Millipore) for 3 minutes until cell detached. We used the culture medium to inhibit enzymatic reaction and centrifuged the suspension at 500×g for 5 minutes, and resuspend the cell pellet in fresh medium.

2.8 Total RNA isolation, RNase R treatment and subcellular localization

Total RNA was extracted using PureLink RNA Mini Kit (Thermo Fisher Scientific) and PureLink DNase Set (Ambion). Total RNAs of normal 10 human tissues were obtained from Ambion Inc. For RNase R treatment, total RNA was incubated with or without RNase R (Epicentre) for 45 minutes at 37 °C to deplete linear and enrich circular RNAs.

To validate the subcellular localization preference, we used the NE-PER nuclear and cytoplasmic extraction reagents (Thermo Fisher Scientific) to separated nuclear and cytoplasmic fractions. Total RNA was then extracted using TRIzol reagent according to

doi:10.6342/NTU202000765

the manufacturer's instructions. qRT-PCR analyses were performed to examine the relative expression of cytoplasmic and nuclear localization for each gene. *GAPDH* and *U6 snRNA* were served as controls for cytoplasmic and nuclear RNAs, respectively.

2.9 cDNA synthesis and RT-qPCR

For mRNA and circRNA quantitation, RNA was reverse-transcribed into cDNA using SuperScript III First-Strand Synthesis System (Thermo Fisher Scientific). QRT-PCR was performed using Luminaris Color HiGreen High ROX qPCR Master Mix (Thermo Fisher Scientific). Quantity of gene expression was normalized by *GAPDH*. For miRNA quantitation, cDNA synthesis was carried out by or miRCURY LNA RT Kit (Qiagen). QRT-PCR was performed by miRCURY LNA SYBR Green PCR Kit (Qiagen) with miRCURY LNA miRNA PCR primer (Qiagen) for each candidate miRNAs, and small nuclear U6 RNA served as an internal standard. QPCR was performed using the StepOnePlus Real-Time PCR System (Applied Biosystems). The primers are provided in Table 4. qRT-PCR reactions were performed using two independent biological replicates, with each having three technical replicates.

doi:10.6342/NTU202000765

Table 4. Sequences of primers used in this study.

# Primer sequences used in qRT-PCR		
Name	**Forward**	**Reverse**
GAPDH	TCAATGACCCCTTCATTGACC	GCATCGCCCCACTTGATTT
circARID1A	CAGTCAAGACCCTCCAGCTT	GTCCCTGTTGCTGCGAGTAT
ARID1A	CATATGGCCCTCCTGCCAAG	TGTTTTGCTGGGCATTGGTG
CCDC91	GGTGGAAGTGGTGAAACCCA	GAAGAGTGGTCACGGTCCAG
FER	ATACACAGGGACCTTGCTGC	TAAGAGCTTCCGGTGCTGTC
HSD11B1	GCGCAAAAGCATGGAAGTCA	CACTTTCCCAGCCAGAGAGG
NLGN1	AGAGCAGTGATGGCATGCTT	CCAGTGGGTCCACATCATCC
PECR	GGAGCTGGGGAGTAATGTGG	CCTGCTTTGTGGGAGGTAGG
RLIM	AGGACAGAGACCTCCAACCA	ACCGAGTTCTGCTGGCTATG
STAG1	ACAGGGACATCGCACTTCTG	TTTTCCACTGAGGTCCAGGC
TOMM20	GAGAGAGCTGGGCTTTCCAA	TGTCAGATGGTCTACGCCCT
UBA6	GCCAACAATGGTGGTACAGG	TGTCTGGAGCAAATGACACAGT
USP45	GCTGACAGTGAGCCTTCAGA	GGTAAAGGGGTCCATCTGGC
VIP	TCTTGGGTCAACTTTCTGCC	CCTCACTGCTCCTCTTTCCATT
VLDLR	ACTTCGTGTGCAACAATGGC	GCGGCATGTTCTCATATGGC
FN1	CTGGCCAGTCCTACAACCAG	ATGAAGCACTCAATTGGGCA
# Primer sequences used in Sanger sequencing		
Name	**Forward**	**Reverse**
Circule3	TATCCCAATGTTCTCGGCCT	CGACGGTATCGATAAGCTTGGA
Luc_circARID1A	AGGTGGGCAAGATCAAGGGG	CCTATTGGCGTTACTATG
# miRCURY LNA miRNA primer sequences used in qRT-PCR		
Name	**Cat. No.**	**Company**
U6 snRNA	YP00203907	Qiagen
hsa-miR-204-3p	YP02113689	Qiagen
# Primer sequences used in site-directed mutagenesis		
Name	**Forward**	**Reverse**
mir204_BindingSite_1	CCCAGCAAACTGCCTATTCGGTCCAGCGCTTCCCTCCACCGCAG	CCTGCGGTGGAGGGAAGCGCTGGACCGAATAGGCAGTTTGCTGGG
mir204_BindingSite_2	CGGCTCCATACCCCTCGGTCCAGTCGACGACACAGC	GCTGTGTCGTCGACTGGACCGAGGGGTATGGAGCCG
mir204_BindingSite_3	TACTCCCAGCAGCCATCGGTCCCTCCACATCAGCAGTC	GACTGCTGATGTGGAGGGACCGATGGCTGCTGGGAGTA
mir204_BindingSite_4	CACCCTCGACGCTCTCGGTCCAGGCTGCGTATCCTC	GAGGATACGCAGCCTGGACCGAGAGCGTCGAGGGTG

2.10 Construction of vector

circARID1A overexpressed plasmid was constructed the exon sequence of circARID1A (E2-E3-E4) into Circle3 (pCIRC2) vector[132] (provided by Dr. Laising Yen), which can circularized the transcript to produce circARID1A. The exon sequence of circARID1A was amplified via PCR from the human cortex, and the PCR product was cloned into the Circle3 vector between Mfe-I and Age-I sites.

ReNcell was knockdown of circARID1A by lentivirus carring shRNA targeting the BSJ of circARID1A, and overexpress circARID1A by lentivirus carring circARID1A sequence, respectively. For dual-luciferase assay, ReNcell was transfected by lentivirus

doi:10.6342/NTU202000765

carring dual-luciferase and circARID1A sequence. The lentiviral vectors were constructed by the National RNAi Core Facility at Academia Sinica. All constructs are sequence-verified.

2.11 Cell transfection

Has-miR-204-3p is overexpressed by mimic transfection (Tools) using Lipofectamine RNAiMAX (Invitrogen) for 48 hours. The sequences of oligonucleotides are shown in Table 5. CircARID1A was knockdown by siRNA (MDBio) to target the BSJ, and overexpress by circARID1A overexpressed plasmid in NHA, SH-SY5Y and U118 cells. Transfection of plasmid was carried out using TransIT-LT1 Reagent (Mirus) according to the transfection manufacturer's instructions for 48 hours.

For lentiviral transduction, the lentiviruses were infected into ReNcell at an MOI of 2 with 8 μg/ml polybrene for 24 hours. Transfected cells were selected by 0.25 μg/ml puromycin for 3 days. The efficiency of knockdown or overexpression in stable expressing cell lines was verified by RT-qPCR.

Table 5. Sequences of oligonucleotides used in this study.

# siRNA sequences		
Name	**Sequences**	**Company**
NC siRNA	UUCUCCGAACGUGUCACGUtt	MDBio
siRNA circARID1A	UGCCUCCAUCCAGUCCAAUtt	MDBio
# miRNA mimic sequences		
Name	**Sequences**	**Company**
Scrambled mimic	GGCAGGUCGAGACGGGAGUAA	Integrated DNA Technologies
hsa-miR-204-3p mimic	GCUGGGAAGGCAAAGGGACGU	TOOLS

doi:10.6342/NTU202000765

2.12 Luciferase reporter assays

The luciferase reporter was constructed by subcloning the circARID1A sequence into the Secrete-Pair Dual Luminescence vector (GeneCopoeia). Cells were seeded in 24-well plate 24 hours prior to transfection. By comparing overexpression of miR-204-3p, we used a scramble miRNA mimic in control group. Dual Luminescence vectors that contained circARID1A sequence were co-transfected with miR-204-3p mimic or scramble mimic, respectively, by TransIT-X2 transfection reagent (Mirus). After 48 hours of transfection, cell culture medium were collected. Gaussia luciferase (GLuc) and secreted alkaline phosphatase (SEAP) activities were measured by Secrete-Pair Dual Luminescence Assay System (GeneCopoeia) according to the manufacturer's protocol. The luciferase activity of GLuc was normalized with SEAP.

We mutated miR-204-3p binding sites in the luciferase-circARID1A reporter vector using Quick-Change Lightning Site-Directed Mutagenesis Kit (Agilent Technologies). The four binding sites were selected because they were also identified by MiRanda[190] (version 3.3a). The mutated GLuc-circARID1A reporter was confirmed by Sanger sequencing. The primers used for mutations of these miR-204-3p binding regions were listed in Table 4.

2.13 Microarray analysis

The microarray hybridization and the data collection were performed with the help of Affymetrix GeneChip System Service center in Genomics Research Center, Academia Sinica. The assessment of purity and integrity of RNA were evaluated by 2100

doi:10.6342/NTU202000765

Bioanalyzer (Agilent Technologies). Total RNA was hybridized to Affymetrix Human Genome Plus 2.0 Array (Affymetrix). The microarray raw data was analyzed using Transcriptome Analysis Console (TAC 4.0) software (Affymetrix). The microarray results of the target genes affected by circARID1A and miR-204-3p are provided at GitHub (https://github.com/TreesLab/circRNA_ASD/tree/master/Microarray_data).

2.14 Neuronal differentiation and Immunostaining

For differentiation of ReNCell into neurons and glial cells, ReNcell was incubated with maintenance medium without containing FGF-2 and EGF growth factors. Maintenance basal media was changed every 3 days for 2 weeks. After 2 weeks, we categorized the neuronal subtypes by immunofluorescence. Cells were plated on glass slides coated with laminin overnight. Cells were fixed with 4% formaldehyde at 37 ^{o}C for 25 min, permeabilized with 0.05% Triton X-100 for 15 min, and incubated with 3% FBS for blocking for 1 hr. Cells were then incubated with primary antibody against MKI67 (cell proliferation marker, cat. no. ab15580, Abcam) βIII-tubulin (neuronal marker; ab18207, Abcam) or GFAP (glial marker; cat. no. 13-0300, Invitrogen) at 4^{o}C overnight. Next day, cells were incubated with fluorescently labeled secondary antibodies at 37^{o}C for 1.5 hours. Nuclei were stained with SlowFade Diamond Antifade Mountant with DAPI (Invotrogen). Details for the antibodies are provided in Table 6.

Table 6. The antibodies used for immunofluorescence.

Antibodies	Host	Cat. No.	Company	Dilution
MKI67	Rabbit	ab15580	Abcam	1:1000
βIII-tubulin	Rabbit	ab18207	Abcam	1:500
GFAP	Rat	13-0300	Invitrogen	1:1000
Alexa Fluor 594 Anti-Rat IgG	Goat	A-11007	Invitrogen	1:200
Alexa Fluor 488 Anti-Rabbit IgG	Goat	111-545-144	Jackson ImmunoResearch	1:200

doi:10.6342/NTU202000765

2.15 Statistical analysis

The data were presented as mean ± standard deviation. Statistically significant differences were calculated using Student's *t*-test, LME and Pearson's correlation, as appropriate. In all cases differences were defined statistically significant when p values < 0.05. A single * indicates $p < 0.05$, ** indicates $p < 0.01$, and *** indicates $p < 0.001$. NS indicates not significant ($p > 0.05$).

2.16 Code availability

The code for the DE-circRNA analysis, the related input data and results were publicly accessible at GitHub (https://github.com/TreesLab/circRNA_ASD).

doi:10.6342/NTU202000765

CHAPTER 3. Results

3.1 Identification of circRNAs in autism and healthy cortex

To assess the potential role of circRNAs, we retrieved 236 total RNA-seq data of temporal cortex, frontal cortex and cerebellar vermis from individuals with ASD and non-ASD (CTL)[9]. First, we characterized circRNA transcripts using NCLscan, which was reported to exhibit the greatest precision among currently accessible circRNA-detection tools[153,154,162,163]. To improve accuracy, we removed the number of detected circRNAs of this sample was less than one standard deviations away from the mean. In total, 53,427 circRNAs were identified in 202 remained samples. Comparison of the number of detected circRNAs per million mapped reads between ASD and CTL samples, there were no statistically significant differences between three brain regions (Fig. 4).

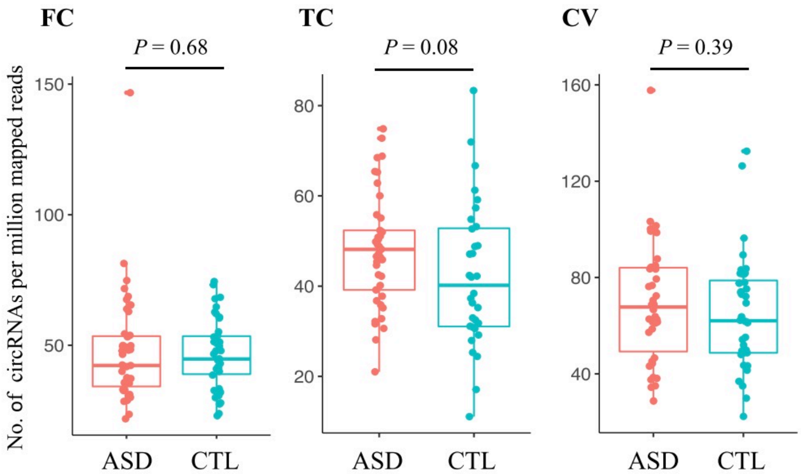

Figure 4. Comparison of normalized numbers of circRNAs in ASD and non-ASD control samples from different brain regions.

Temporal cortex; TC, Frontal cortex; FC, cerebellar vermis; CV. *P* values were determined by two-tailed Wilcoxon rank-sum test.

doi:10.6342/NTU202000765

Of the 134 cortex (TC and FC) samples, 36,624 circRNA events were detected, 40% were found in one sample only. To reduce potentially spurious events, we only remained the circRNAs detected in more than 50% of the 134 samples. After filtering, a total of 1,060 circRNAs were considered for the following analyses (Fig. 5).

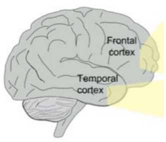

	ASD	CTL	Sum
Frontal cortex (FC)	37	36	**73**
Temporal cortex (TC)	36	25	**61**
Total no. of RNA-seq			**134**

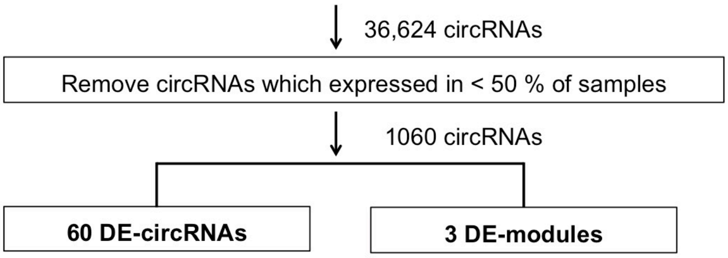

Figure 5. The workflow of the identification of DE-circRNAs and DE-modules.

Of note, 61.4% of the 1,060 circRNAs were detected in mouse and 47% were observed in mouse brain (Fig. 6), indicating that circRNAs were highly conserved between human and mouse.

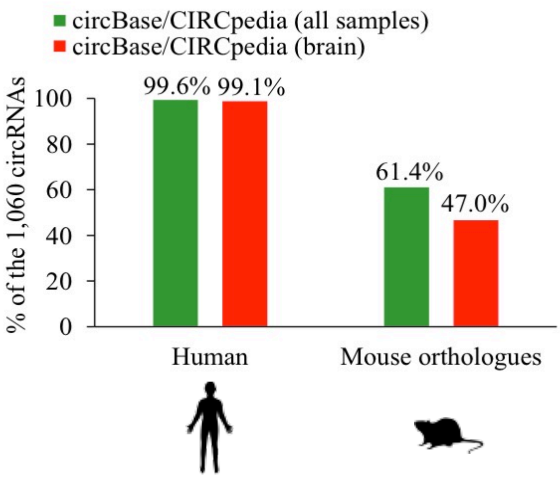

Figure 6. Comparisons of the 1,060 circRNAs and human/mouse circRNAs collected in the well-known databases.

doi:10.6342/NTU202000765

The principal component analysis (PCA) was performed on 1,060 circRNAs, which revealed that circRNA expression profiles were very similar between two cortex regions but were quite distinct in the cerebellum vermis (Fig. 7). This result is consistent with previous observations for mRNAs[15,191], miRNAs[64] and circRNA. Since several independent transcriptomics studies of ASD have indicated that human cortex has been implicated in ASD pathophysiology[160,161] and changes in transcriptomic profiles were stronger in the cortex than in the cerebellum[16]. So, here we focus our analysis of circRNA dysregulation on frontal and temporal cortex samples from ASD and non-ASD individuals.

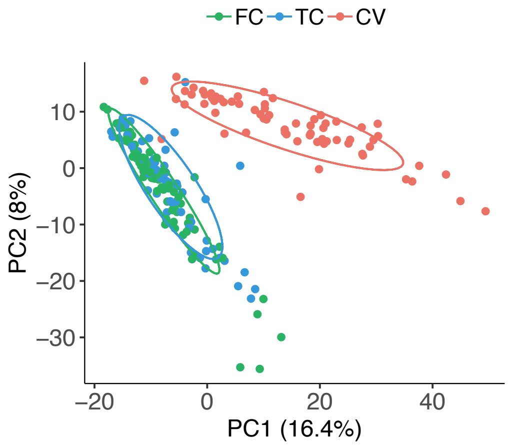

Figure 7. Principal component plots of circRNA expression profiles of the 1,060 circRNAs in samples from FC, TC, and CV.

PC1/PC2, the first and second principal components.

3.2 Differential expression of circRNAs in ASD cortex

We used linear mixed effects (LME) model to detect differentially expressed (DE)-circRNAs between ASD and non-ASD samples with controlling for confounding factors, including sex, age, brain region, RIN, PMI, host gene expression, sequencing

doi:10.6342/NTU202000765

batch, and brain bank batch. Then total of 60 DE-circRNAs were identified by LME algorithms ($p < 0.05$ & | log2 (fold change) | > 0.5), among which 22 were upregulated and 38 were downregulated in ASD cortex (Fig. 8).

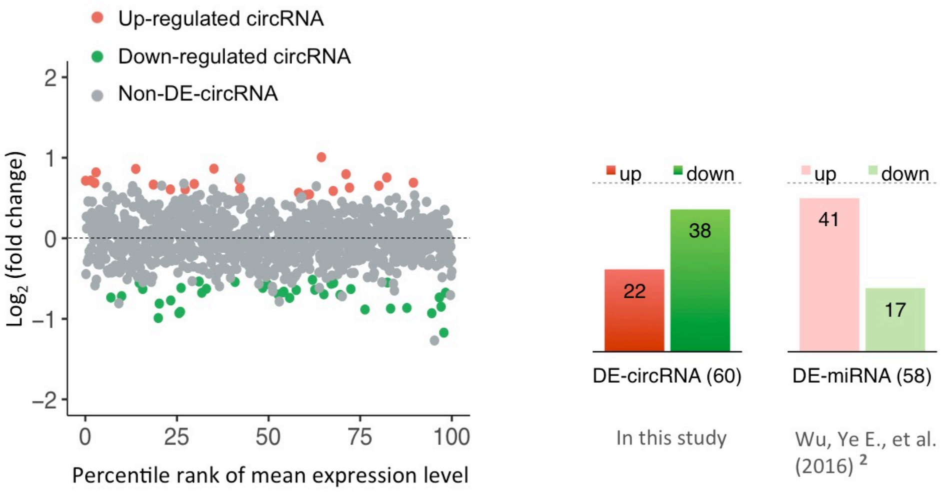

Figure 8. DE-circRNAs between ASD and CTL cortex.

Plotted against the percentile rank of mean expression levels of the 1,060 circRNAs across 134 cortex samples used for differential expression analysis. The identified 22 upregulated and 38 downregulated circRNAs in the ASD cortex samples are highlighted in red and green, respectively. Previous study evaluated 41 upregulated and 17 downregulated miRNAs in ASD cortex.

Then, we used resampling analysis with 100 replacement (bootstrapping) of random sampling of 70% of the samples examined in order to estimate the robustness of the 60 DE-circRNAs. The fold changes of DE-circRNAs for the resampled sets and the original sample sets were highly concordant (Fig. 9).

doi:10.6342/NTU202000765

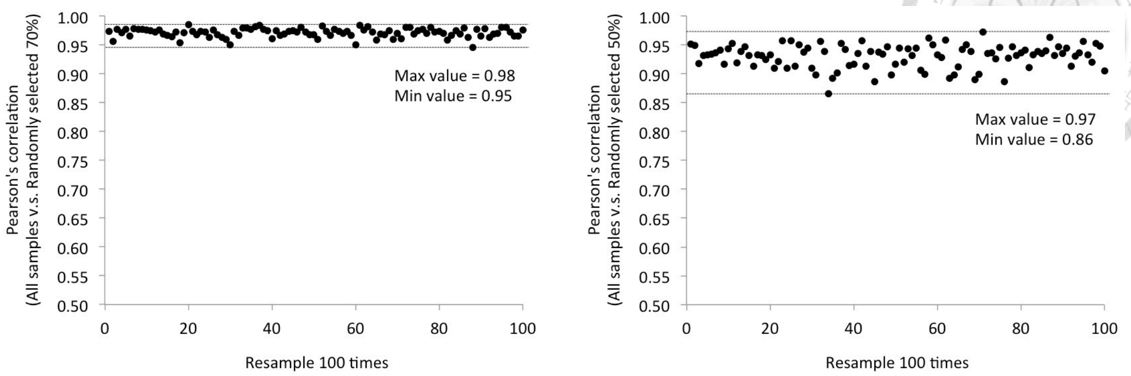

Figure 9. Resampling analysis with 100 rounds of random sampling of 70% and 50% of the samples examined.

The fold changes of the 60 DE-circRNAs for the resampled and the original sample sets were highly concordant between each other. The Pearson correlation coefficients (*R* value) between 0.95 and 0.98, all $p < 2.2\times10^{-16}$).

We found that the fold changes for the 60 DE-circRNAs were concordant between the FC and TC (Fig. 10). In addition, we compared the fold changes of DE-circRNAs for a small number of samples with those for all samples, and found a high concordance between each other. These observations revealed that our results were not biased by a small number of samples with removal of Chromosome 15q11-13 duplication (dup15q) syndrome, low RIN (≤ 5), or high PMI (≥ 30h) (Fig. 10).

doi:10.6342/NTU202000765

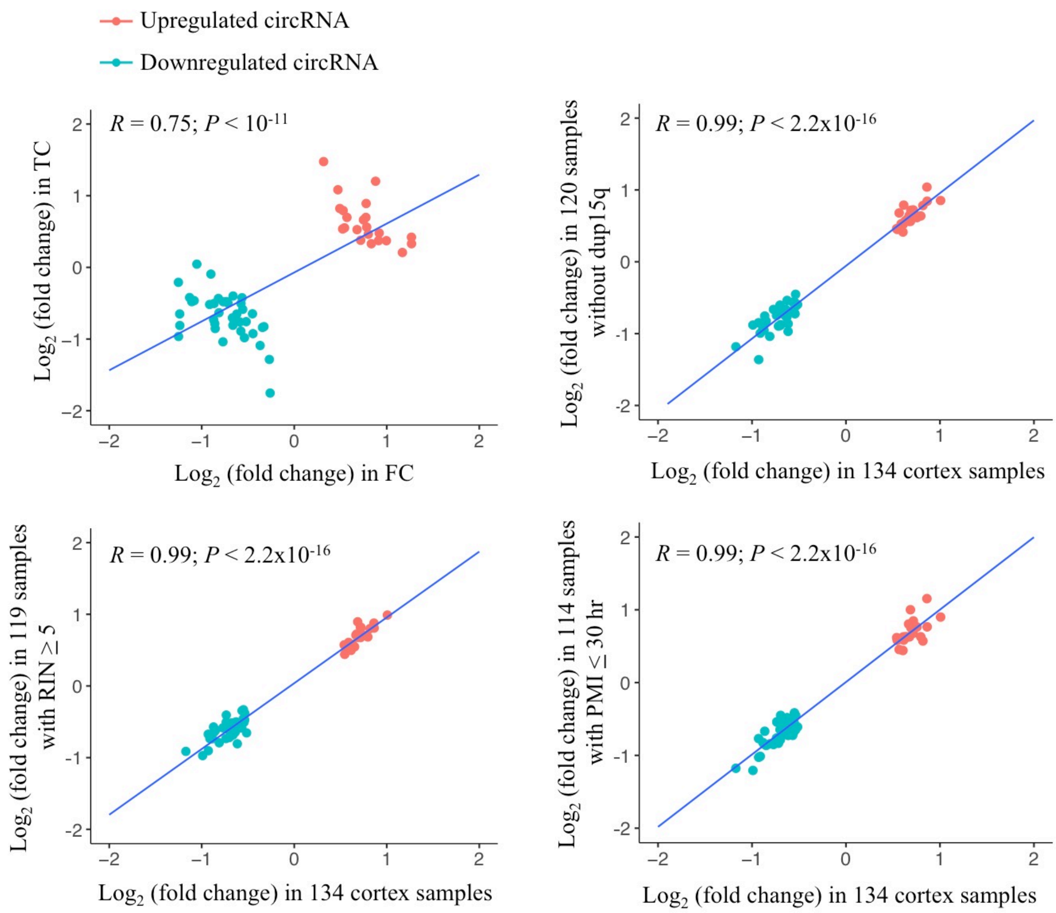

Figure 10. Comparison of DE-circRNA expression fold changes in the FC and TC samples and the corresponding small number of samples and all 134 samples combined.

The blue lines represent the regression lines.

The PCA result revealed that ASD and non-ASD samples could be distinguished into separate clusters based on the identified DE-circRNAs (Fig. 11A). However, ASD and non-ASD samples cannot be separated by the host genes of DE-circRNA (Fig. 11B) or 1060 identified circRNAs (Fig. 11C).

doi:10.6342/NTU202000765

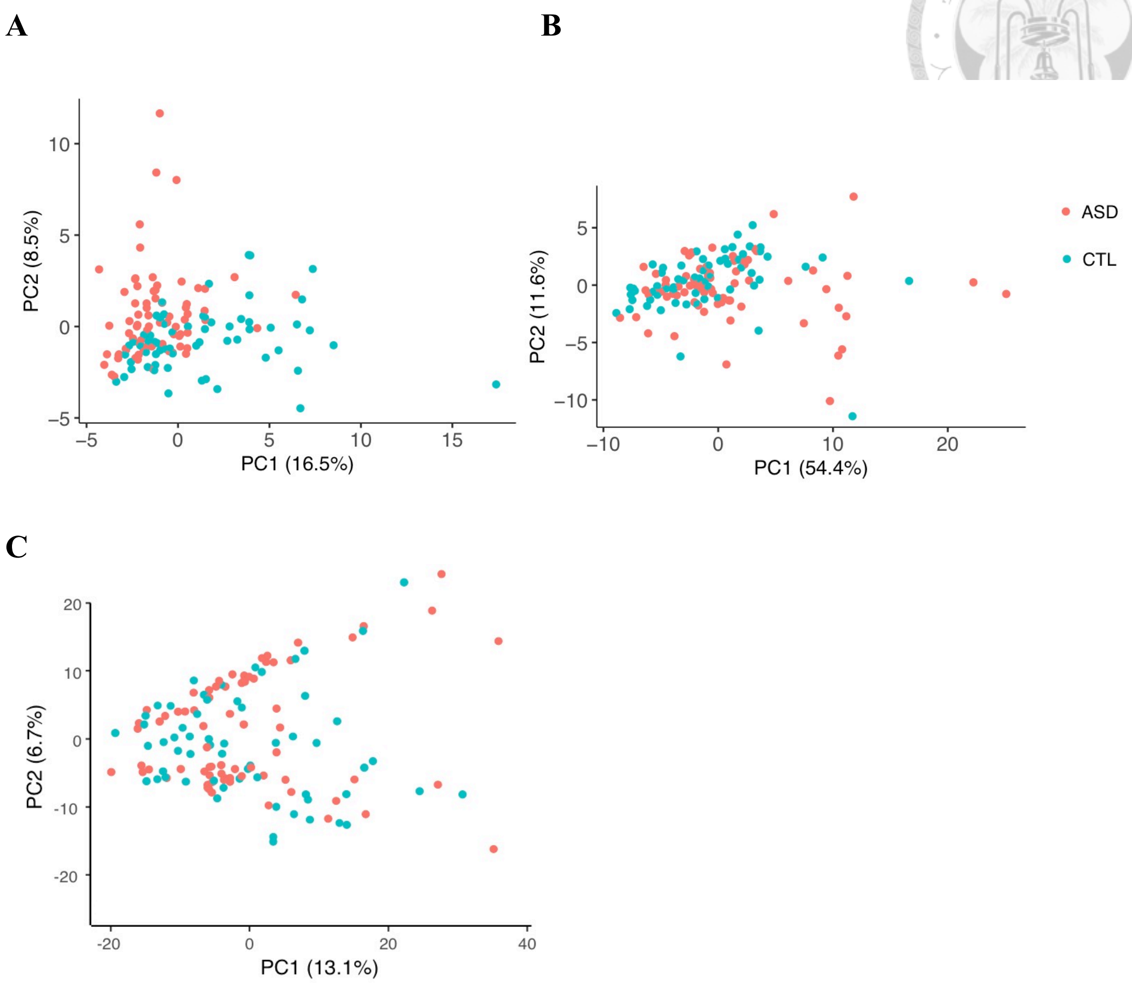

Figure 11. PCA based on the 60 DE-circRNAs and their host genes in ASD and non-ASD samples.

(A) PCA based on the 60 DE-circRNAs; (B) PCA based on the 60 DE-circRNAs of host genes; (C) PCA based on 1060 identified circRNAs.

Furthermore, hierarchical clustering based on the 60 DE-circRNAs showed distinct clusters for the majority of ASD samples. For the clustering of the 134 cortex samples, two distinct clusters were observed: 76% (44 out of 58) and 38% (29 out of 76) of cortex samples were ASD samples in the right and left clusters, respectively (*P* value < 0.0001 by two-tailed Fisher's exact test) (Fig. 12). However, the confounding factors did not drive the similar clustering. Our result revealed a shared circRNA dysregulation signature among the majority of ASD samples.

doi:10.6342/NTU202000765

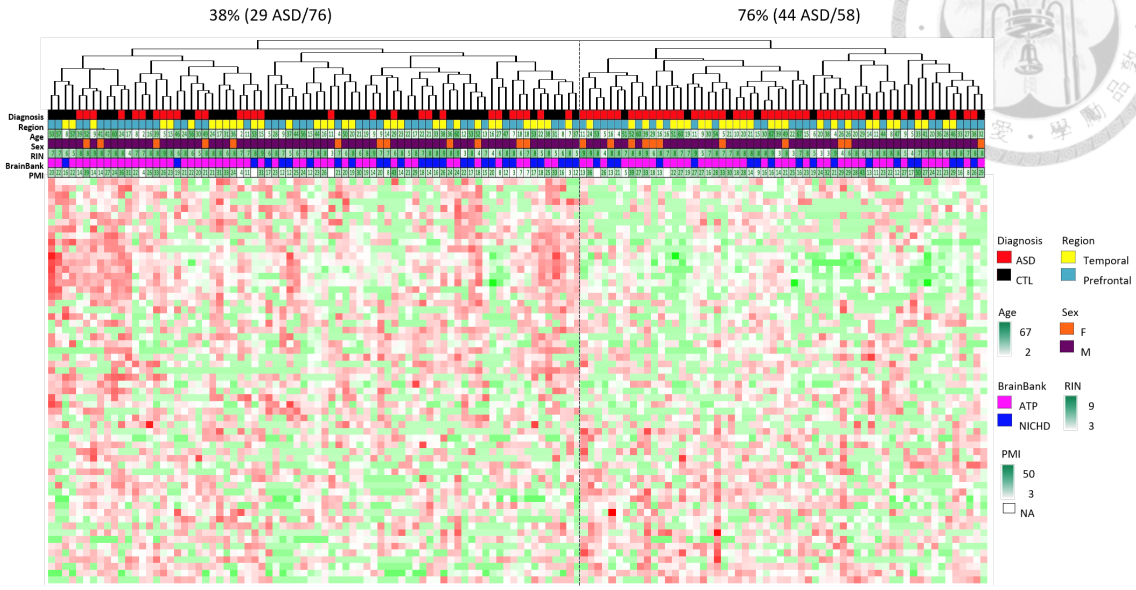

Figure 12. Clustered heatmap of 60 DE-circRNAs in ASD and non-ASD.

Dendrogram representing hierarchical clustering of 134 cortex samples based on the identified 60 DE-circRNAs. Information on diagnosis, age, brain bank, PMI, brain region, sex, and RIN is indicated with color bars below the dendrogram according to the legend on the right. Heat map on the bottom represents scaled expression levels (color-coded according to the legend on the right) for the 60 DE-circRNAs.

3.3 Construction of co-expression networks of circRNA dysregulation in ASD

To probe the correlation between circRNA expression changes and disease status at the system level, we performed the weighted gene co-expression network analysis (WGCNA)[80,81] on 1,060 circRNAs identified from the 134 cortex samples. As shown in Figure 13, we identified 14 modules and estimated the module eigengene, that is, the first principal component (PC1) of the module's circRNA expression.

doi:10.6342/NTU202000765

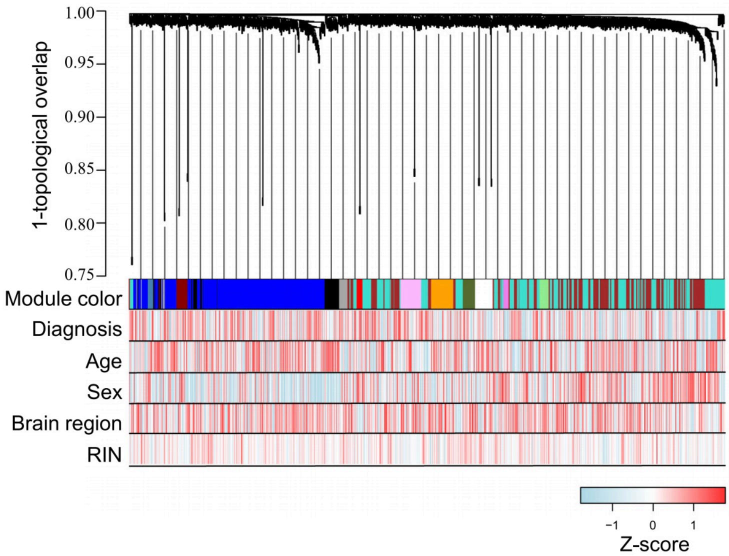

Figure 13. Hierarchical cluster tree showing 14 modules of co-expressed circRNAs.

Consensus module color bars shows assignment based on 1,000 rounds of bootstrapping. Diagnosis and potential confounders (age, sex, region, RIN) are treated as numeric variables to calculate their Pearson correlation coefficients with expression level for each circRNA.

By assessing relationship of module to diagnosis status, three modules (dark red, violet, and turquoise; designated as "DE-modules") were significantly correlated with ASD status (Fig. 14A). Of note, the three modules were not correlated with experimental covariates (age, sex, and brain region) and technique confounders (RIN, PMI, and brain bank). The upregulated dark red module contains 21 circRNAs, and the downregulated violet module contains 10 circRNAs and turquoise module contains 288 circRNAs, respectively (Fig. 14B).

doi:10.6342/NTU202000765

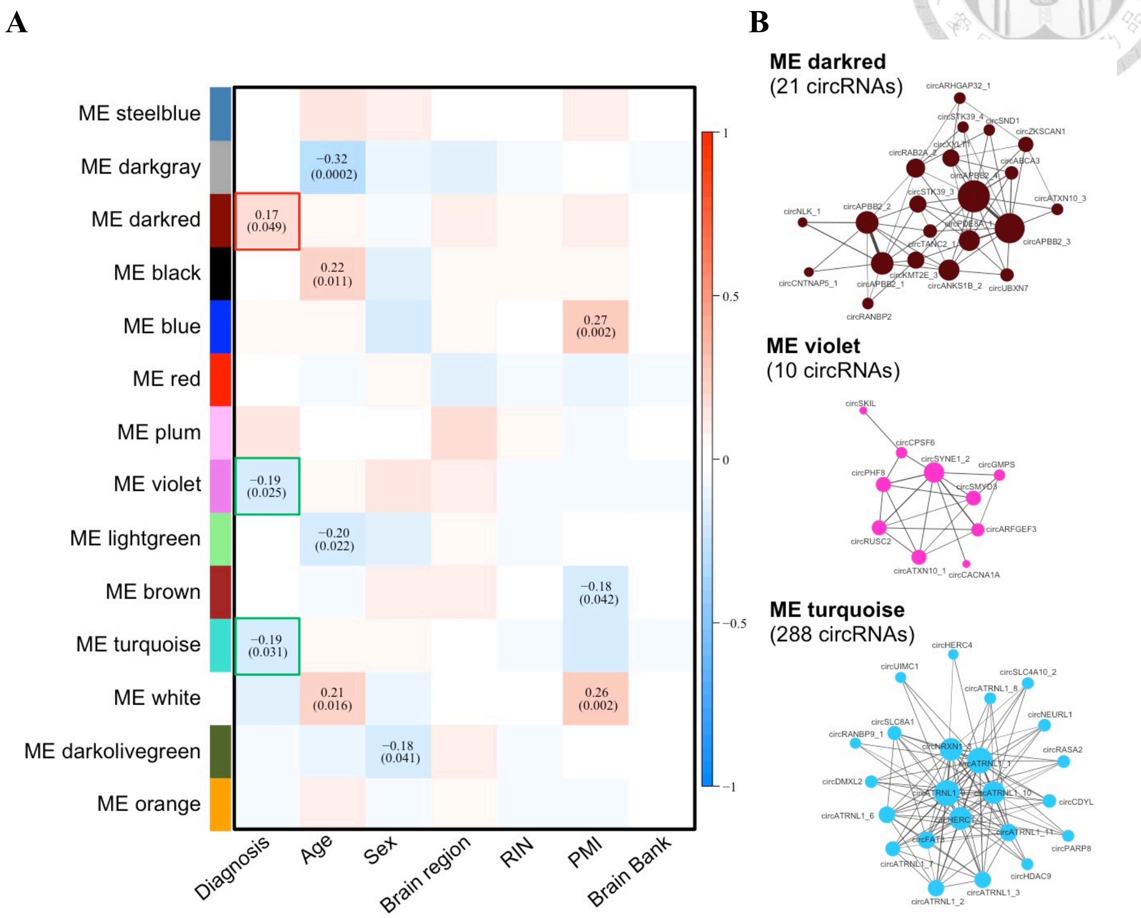

Figure 14. Dysregulation of circRNA coexpression networks in ASD cortex.

(a) Module-covariates associations. The colour scale shows module-covariates correlation from -1 (blue) to 1 (red). (b) The subnetwork of circRNA expression correlations in the module, where the circRNAs in violet and darkred modules are all plotted, but the circRNAs in turquoise module are plotted with only kME ≥ 0.5 due to the sizable number of circRNAs. Node size is proportional to connectivity, and edge thickness is proportional to the absolute correlation between two circRNAs.

To test the robustness of the three DE-modules, we then asked if the coexpression structure was similar between ASD and non-ASD control samples, and between FC and TC. To this end, we performed the summary preservation statistic[192], a statistics that determined whether a reference network can be found in another test network. Indeed, we observed that the $Z_{summary}$ scores, which were evaluated for each module to measure

doi:10.6342/NTU202000765

the preservation, of all three DE-modules were greater than or equal to two, indicating that the three modules were preserved across ASD and non-ASD control samples (Fig. 15A) and across FC and TC samples (Fig. 15B). Our results thus support the robustness of the three ASD-associated modules.

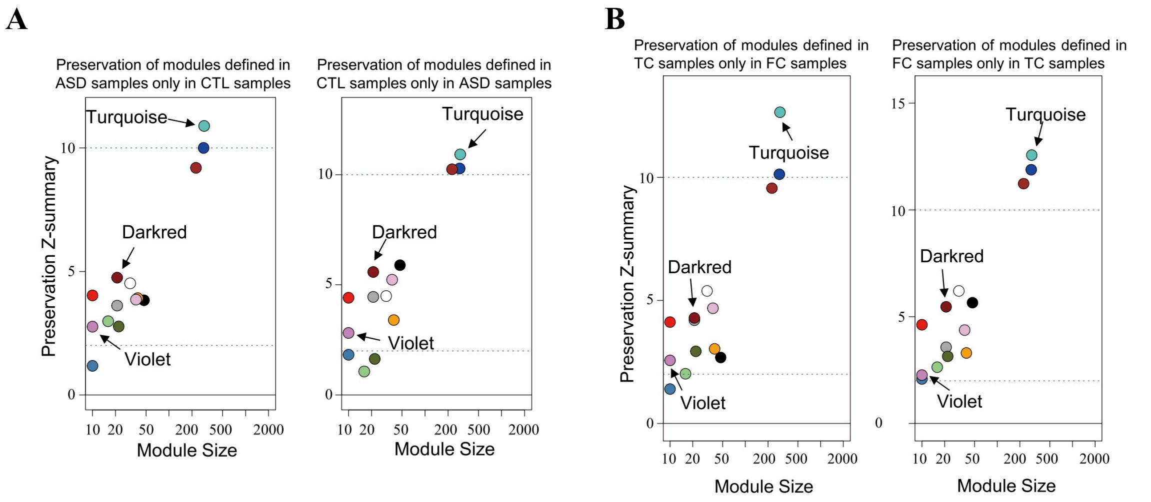

Figure 15. Module preservation Z-summary statistics of 14 modules.

Module preservation defined in ASD samples only in CTL samples (A; left), CTL samples only in ASD samples (A; right), TC samples only in FC samples (B; left), or FC samples only in TC samples (B; right). The horizontal lines indicate each module with a Zsummary threshold for strong evidence of conservation (Zsummary > 10), week to moderate evidence of conservation (2< Zsummary <10), and no evidence conservation (Zsummary < 2).

3.4 Profiling of ASD-associated circRNA–miRNA–mRNA regulatory axes

We have identified 60 DE-circRNAs and three DE-modules in ASD cortex. To further identify the corresponding ASD-associated miRNA–mRNA regulatory interactions that were potentially regulated by ASD-associated circRNAs, we extracted 58 DE-miRNAs in ASD cortex from the study of Wu et al.[12]. These ASD-affected miRNAs were derived from 95 human cortex samples, of which 73 samples overlapped with the samples examined in this study. Since circRNAs often act as a miRNA sponge, we directly

doi:10.6342/NTU202000765

assessed the role of circRNA dysregulation in alterations of the ASD-affected miRNAs. Thus, we searched for the target sites of 41 upregulated miRNAs in 38 downregulated circRNAs and 298 circRNAs defined in two downregulated circRNA modules; and searched for the target sites of 17 downregulated miRNAs in 22 upregulated circRNAs and 21 circRNAs defined in an upregulated circRNA module.

After that, we determined the ASD-associated circRNA–miRNA–mRNA interactions by integrating the identified interactions for circRNA–miRNA and miRNA–mRNA pairs according to the common miRNA target sites of the circRNAs and mRNAs. The ASD-associated circRNA–miRNA–mRNA interactions were constructed by integrating 808 circRNA–miRNA axes with 36,512 miRNA–mRNA axes, we therefore determined 529,509 circRNA–miRNA–mRNA axes according to the common miRNA served as linker between the DE-circRNAs and DE-mRNAs. The circRNA–miRNA–mRNA axes were provided at GitHub (https://github.com/TreesLab/circRNA_ASD).

We then calculated the correlations between circRNA and miRNA expression, between miRNA and mRNA expression, and between circRNA and mRNA expression based on the same set of cortex samples (i.e., 73 samples). As shown in Figure 16, the circRNA–miRNA–mRNA axes were simultaneously satisfied the criteria.

doi:10.6342/NTU202000765

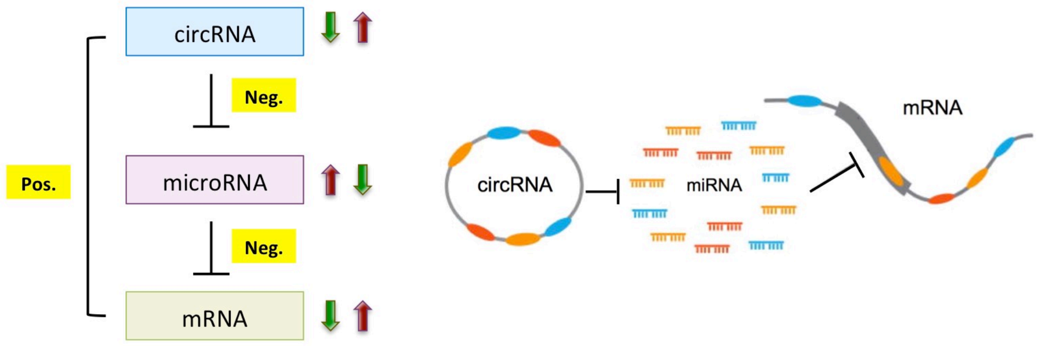

Figure 16. Schematic diagram representing the criteria for the identified ASD-associated circRNA–miRNA–mRNA axes.

Therefore, a total of 8,170 ASD-associated circRNA–miRNA–mRNA axes were determined, including 356 upregulated (Fig. 17A) and 7,814 downregulated (Fig. 17B) circRNA-involved axes. The ASD-affected circRNA may provide an upstream regulation for the ASD-associated miRNA–mRNA pathways and thereby potentially contribute to ASD susceptibility.

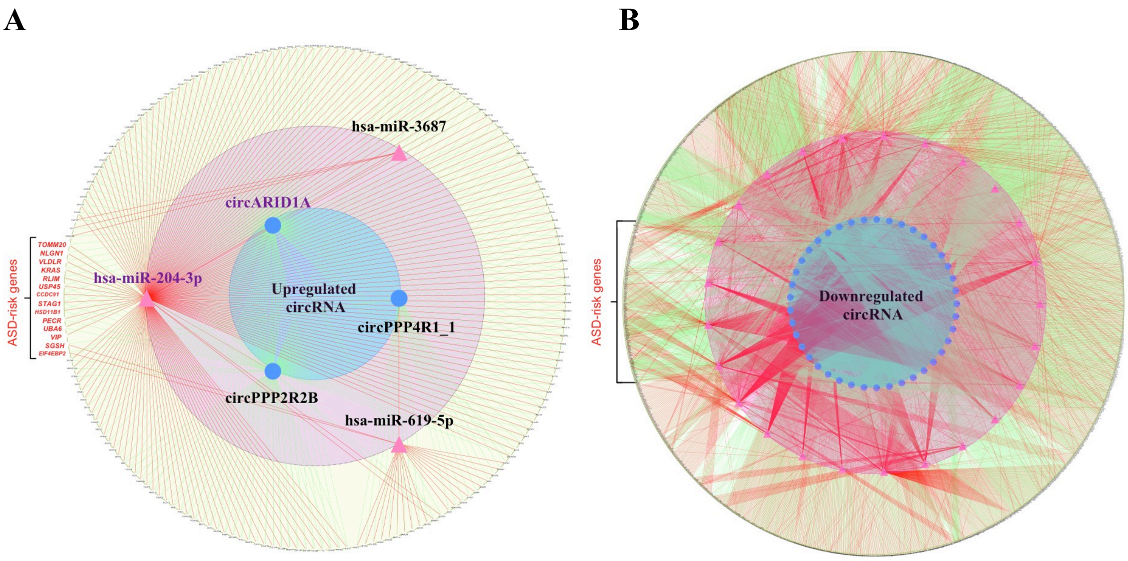

Figure 17. The 8170 ASD-associated circRNA–miRNA–mRNA interactions.

CircRNAs and miRNAs are indicated by blue circle and pink triangle, respectively. The interactions were plotted by Cytoscape software.

doi:10.6342/NTU202000765

We provided 8,170 circRNA–miRNA–mRNA regulatory interactions that potentially contributed to ASD susceptibility for future study. The network contained 46 circRNAs, 30 miRNAs and 2,302 target genes. According to the target genes previously implicated in ASD or the experimental evidence of miRNA–mRNA binding, we further classified the identified circRNA–miRNA–mRNA axes into four categories as follows:

Category 1: The target genes have been previously reported to be ASD risk genes (i.e., SFARI or AutismKB genes).

Category 2: The target genes were reported to be DE-genes in ASD[16] based on the samples overlapped with the samples examined in this study. The interactions should be either upregulated circRNA – downregulated miRNA – upregulated mRNA or downregulated circRNA – upregulated miRNA – downregulated mRNA interactions.

Category 3: The miRNA–mRNA interactions has been experimentally validated.

Category 4: Other.

The 780 axes in category 1, and in which the 188 ASD risk genes may play an important regulatory role in ASD brain. The target genes of the categories 2-4 interactions, which were identified to regulated by upstream ASD-affected circRNA–miRNA axes, may be valuable candidates for further studies in idiopathic ASD (Fig. 18).

doi:10.6342/NTU202000765

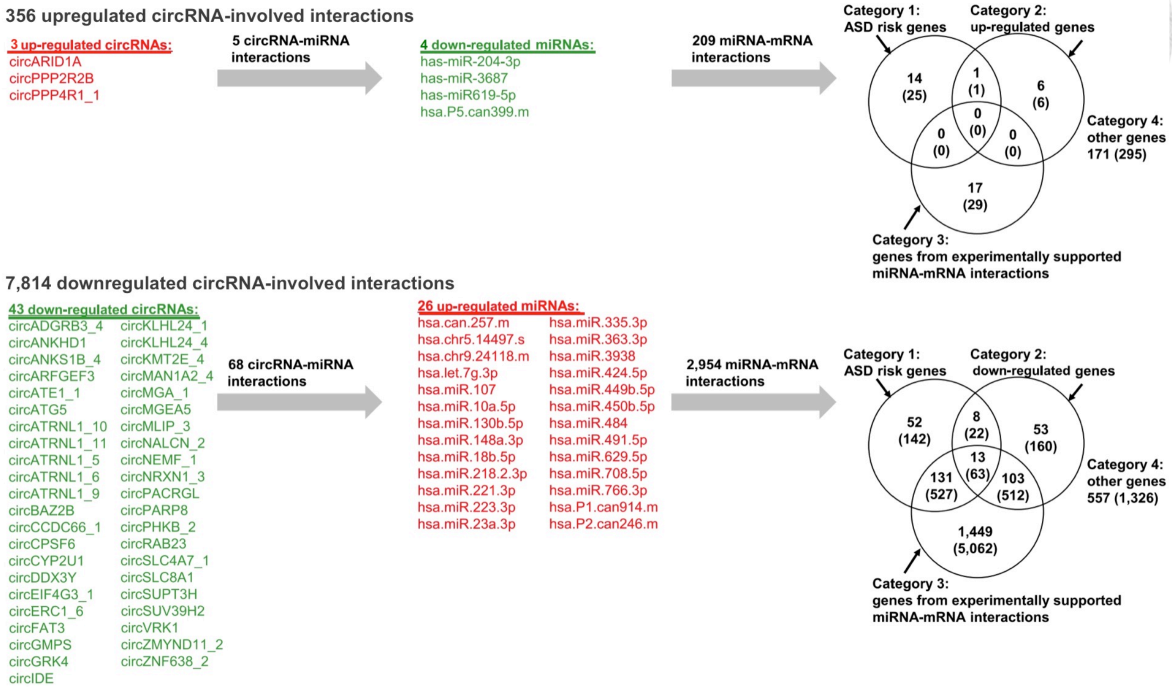

Figure 18. The four categories of circRNA-involved ASD-associated circRNA–miRNA–mRNA interactions.

Venn diagrams represent the overlap between the four categories of interactions, on which the numbers between brackets show the numbers of target genes. The numbers of the identified circRNA–miRNA–mRNA interactions are shown in parentheses.

To explore the relationship between ASD and the 2,302 target genes, we first used the ToppFunn module of ToppGene Suite software[186] to assessed enrichment of target genes for Human Phenotype Ontology terms. We found that the target genes were significantly enriched in the phenotype ontology terms of aplasia/hypoplasia involving the central nervous system (CNS) and abnormality of forebrain, cerebrum, central mortor, and skull size, reflecting the brain morphometry differences between ASD patients and healthy individuals (Fig. 19A).

Regarding the 2,302 target genes, we further examined enrichment for ASD risk genes from Simons Foundation Autism Research Institutive (SFARI)[67] and AutismKB[84]

doi:10.6342/NTU202000765

databases, which have been previously implicated in ASD through genetic syndromes, candidate gene studies, common variant association, and structural variation. The target genes showed significant enrichment for both SFARI and AutismKB genes (particularly for top SFARI genes with score = 1- 3 and syndromic), but not for genes implicated in monogenetic forms of schizophrenia, Alzheimer, intellectual disability and other brain disorders (Fig. 19B). These results suggest that targets of the identified circRNA–miRNA–mRNA interactions are enriched for genes causally connected with autism, but less so far genes connected with other brain disorders. In addition, we found that these target genes were significantly enriched in genes encoding inhibitory postsynaptic density (PSD) proteins, but not in those encoding excitatory PSD ones (Fig. 19B). This result reflects a previous observation that ASD-derived organoids exhibit overproduction of inhibitory neurons[185,193].

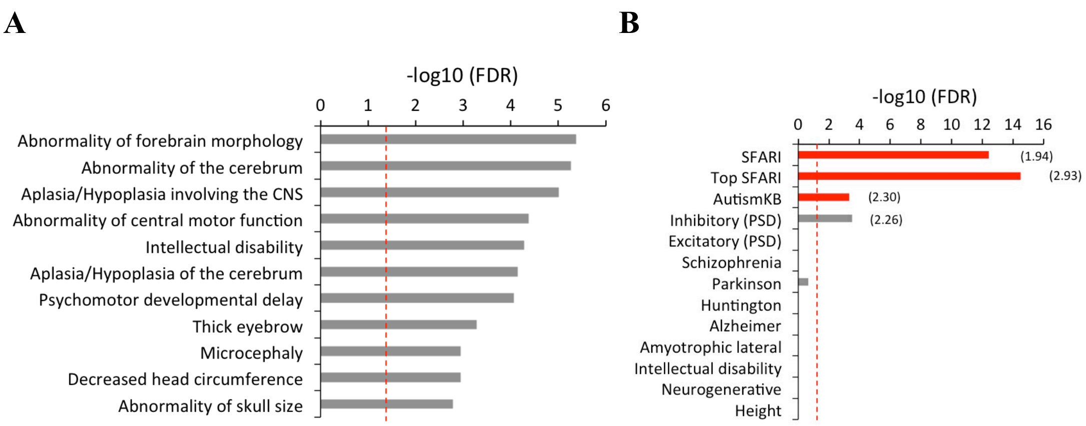

Figure 19. Enrichment analyses of phenotype ontology (A) and 14 group of gene list (B) among the target genes of the identified ASD-associated circRNA–miRNA–mRNA interactions.

The *P* values are determined by two-tailed Fisher's exact test. The red dashed lines represent the adjusted *p*-value (FDR) < 0.05. The enrichment odds ratios with FDR < 0.05 are provided in parentheses.

doi:10.6342/NTU202000765

3.5 Experimental validation of circARID1A interacting with miR-204-3p

As previously mentioned, circRNAs could function as miRNAs sponge. To investigate the interaction between dysregulated circRNA and miRNA in ASD, we predict DE-miRNA binding sites on DE-circRNAs that have been identified in the same ASD samples used in this study. Then, we selected a circARID1A that was back-spliced from exon 2-4 of ARID1A (chr1: 26,729,651–26,732,792) (Fig. 20A). CircARID1A was predicted to have the greatest number of target sites of DE-miRNAs (miR-204-3p) using the software RNA22[172] (version 2.0) with default parameters (Fig. 20B). The circARID1A was significantly upregulated in ASD samples (Fig. 20C).

A

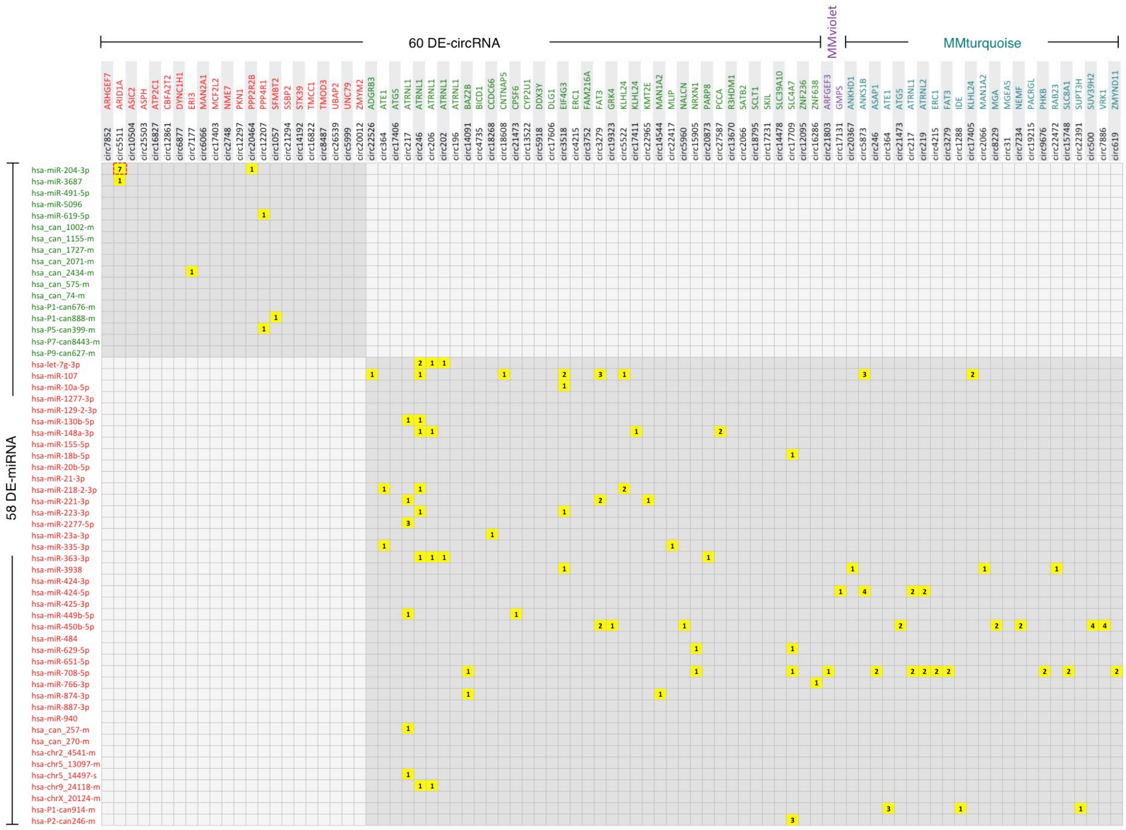

doi:10.6342/NTU202000765

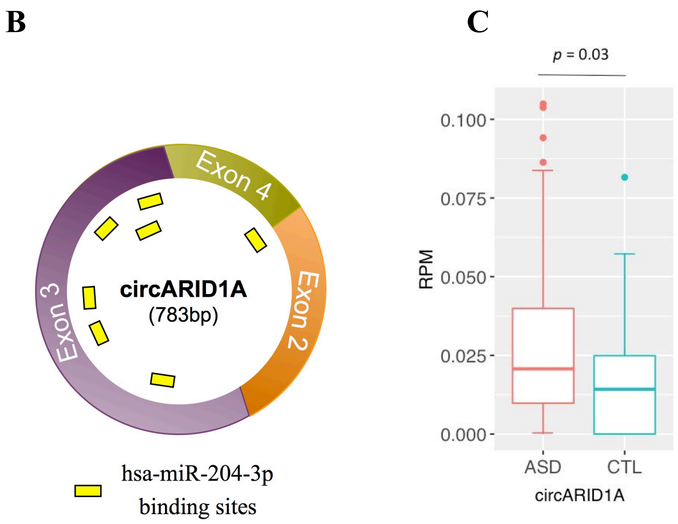

Figure 20. CircARID1A serves as a sponge for miR-204-3p.

(A) Numbers of the predicted binding sites of the previously identified DE-miRNAs in ASD on the DE-circRNA and circRNA modules. Only the circRNA–miRNA regulatory axes with a significantly negative correlation are shown. Upregulated and downregulated miRNAs/circRNAs are highlighted in red and green, respectively. The red square highlights circARID1A that was predicted to have seven target sites of miR-204-3p. (B) Schematic illustration seven predicted target sites of miR-204-3p on circARID1A. (C) Comparison of the expression of circARID1A in 134 cortex samples.

Here, the NCL junction of circARID1A has not yet been experimentally confirmed previously. The roles of both circARID1A and miR-204-3p and their regulatory interaction in CNS have not yet been investigated. We first confirmed the BSJ of circARID1A by divergent primers, which designed around the NCL junction of circARID1A. The primers are provided in Table 4. Since comparisons of different reverse transcriptase RTase products have been demonstrated to effectively detect RT-based artificially NCL junctions[30,89-92]. We performed RT-PCR using MMLV- and AMV-derived RTase in parallel experiments (Fig. 21A), and PCR amplification of NCL junction validated by Sanger sequencing (Fig. 21B). Our result demonstrated that the NCL junction of circARID1A was RTase-independent, supporting that the NCL junction was unlikely to be generated by an RT-based artifact.

doi:10.6342/NTU202000765

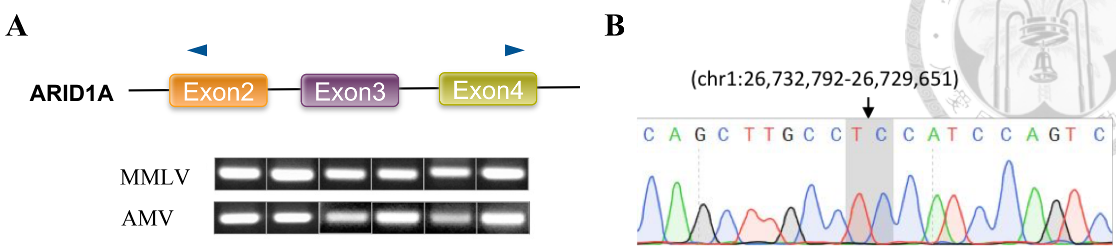

Figure 21. Validation of the back-spliced junction of circARID1A through RT-PCR and Sanger sequencing.

(A) Comparisons of two different RTase products of circARID1A in TC/FC samples and four types of neuronal cell lines (ReN, NHA, SH-SY5Y, and U118). (B) Backsplicing site of circARID1A was confirmed by Sanger sequencing in the TC and ReNcell.

Subsequently, we treated total RNA from the examined cell lines/tissues with RNase R. RNase R was used to confirm the existence of circRNAs. As expected, circARID1A was resistant to RNase R treatment, while linear ARID1A was significantly reduced in cell treated with RNase R, supporting the existence of the circARID1A (Fig. 22).

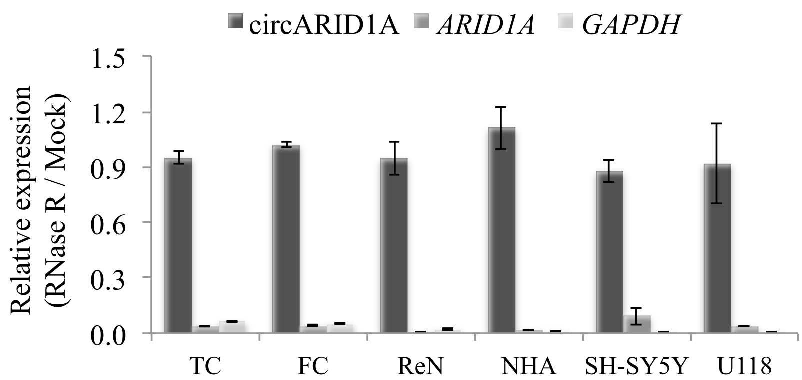

Figure 22. Resistance of circARID1A, *ARID1A* and *GAPDH* after the RNase R treatment.

The percentage of RNA remaining was before and after RNase R treatment in the indicated tissues/cell lines determined by qRT-PCR. *GADPH* was served as negative controls.

doi:10.6342/NTU202000765

Intriguingly, we observed that circARID1A was commonly expressed across the brains of vertebrate species from primates to chicken, indicating the evolutionary significance of circARID1A (Fig. 23).

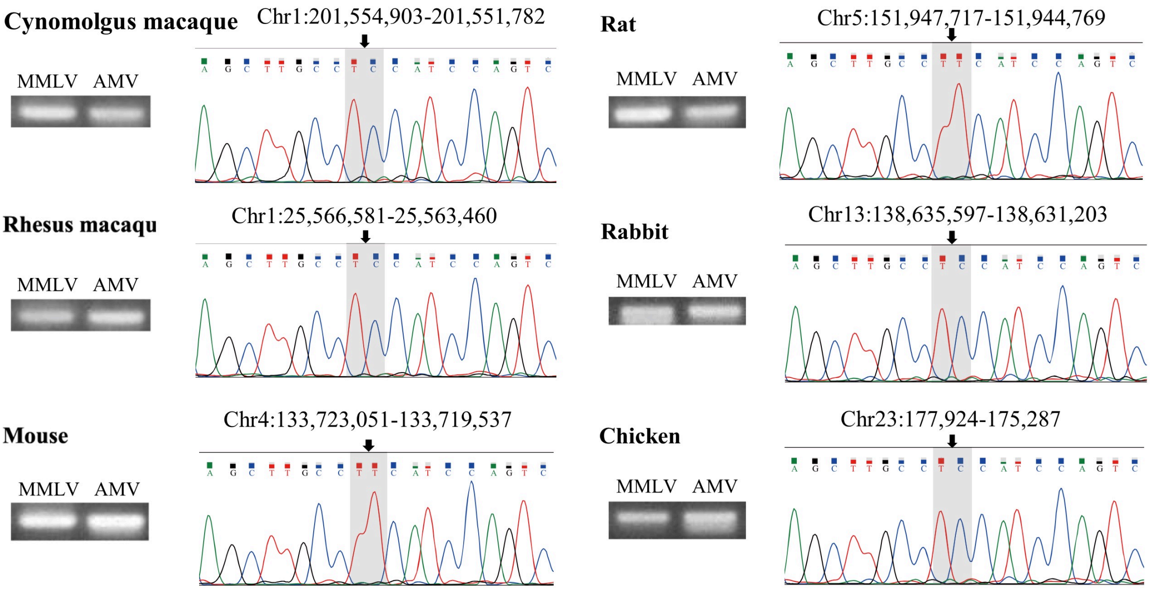

Figure 23. Experimental examination of the evolutionary conservation of circARID1A across vertebrate brains.

Comparison of MMLV- and AMV-derived-RTase products and the corresponding sequence chromatograms for the circARID1A event in the brains of the indicated six species.

We examined the expression profiles of circARID1A and its corresponding colinear mRNA counterpart in various human tissues. The result showed these two isoforms exhibited different expression patterns. CircARID1A was particularly enriched in brain, whereas its corresponding mRNA counterpart was not (Fig. 24A). Importantly, regarding the relative expression of these two isoforms in the brain, circARID1A was significantly more abundant than its colinear form; in contrast, circARID1A was expressed at a relatively low level as compared to its colinear form in the non-brain tissues (Fig. 24B)

doi:10.6342/NTU202000765

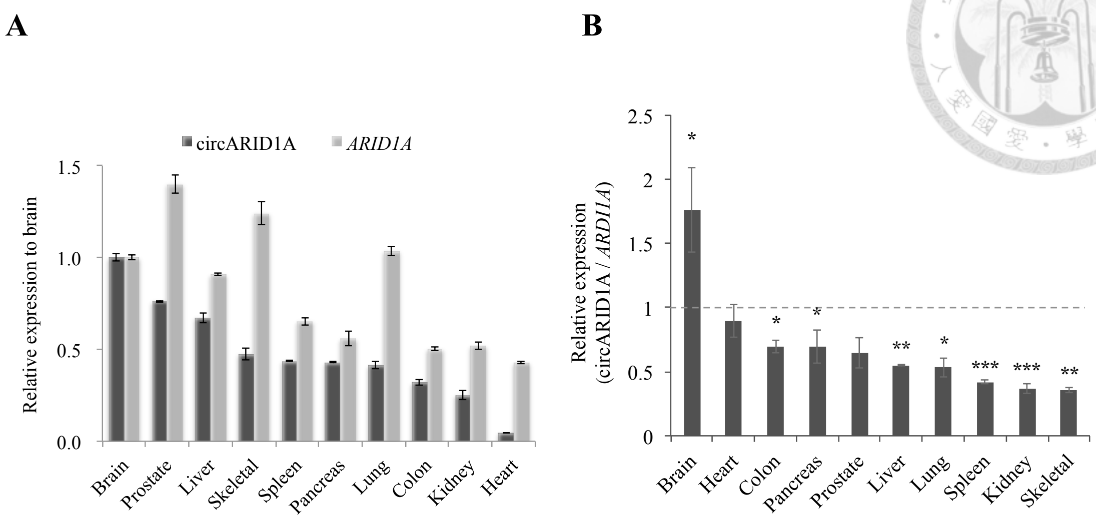

Figure 24. The relative expression of circARID1A and its corresponding co-linear mRNA counterpart in 10 normal human tissues.

(A) The expression levels of brain are used to normalize the relative expression values of the other tissues. (B) The relative expression of circARID1A and ARID1A in 10 normal human tissues.

We also demonstrated that circARID1A was widely expressed in 24 human brain regions by Human Brain cDNA Array (OriGene). These results thus suggested the biological importance of circARID1A in human brain (Fig. 25).

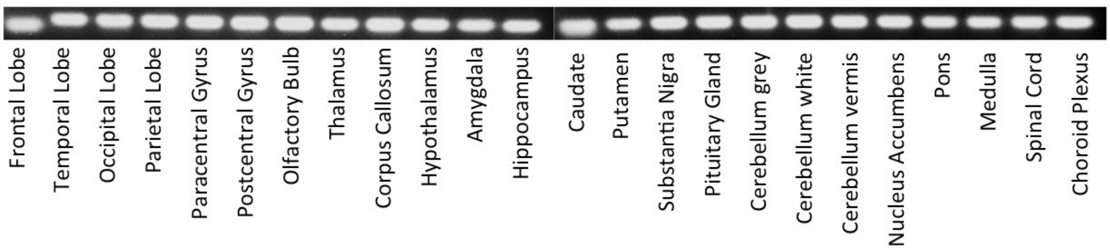

Figure 25. RT-PCR analysis of circARID1A expression in 24 human brain regions.

To function as a miRNA sponge, circRNAs not only need to harbor miRNA-binding sites but also be expressed at high levels in the cytosol. To test if circARID1A plays a

doi:10.6342/NTU202000765

regulatory role of miR-204-3p activities, we confirmed that circARID1A was indeed predominantly expressed in the cytoplasm in both ReN and NHA cells (Fig. 26).

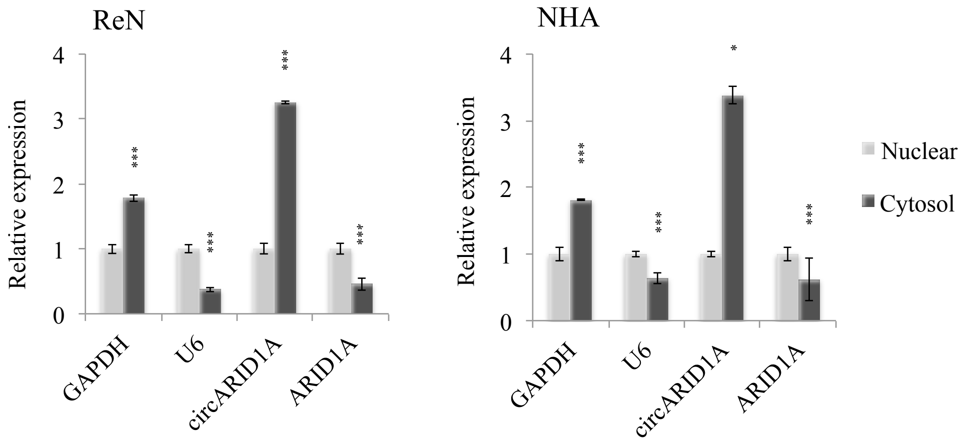

Figure 26. Subcellular localization of circARID1A and ARID1A.

The expression levels in nucleus are used to normalize the relative expression values in cytoplasm. GAPDH and U6 snRNA are examined as a cytosol marker and a nucleus marker, respectively.

To investigate the downstream effect of circARID1A, knockdown and overexpression of circARID1A in different types of neuronal cell lines were established. We found that circARID1A knockdown and overexpression did not significantly affect the expression of its corresponding colinear mRNA counterpart (Fig. 27).

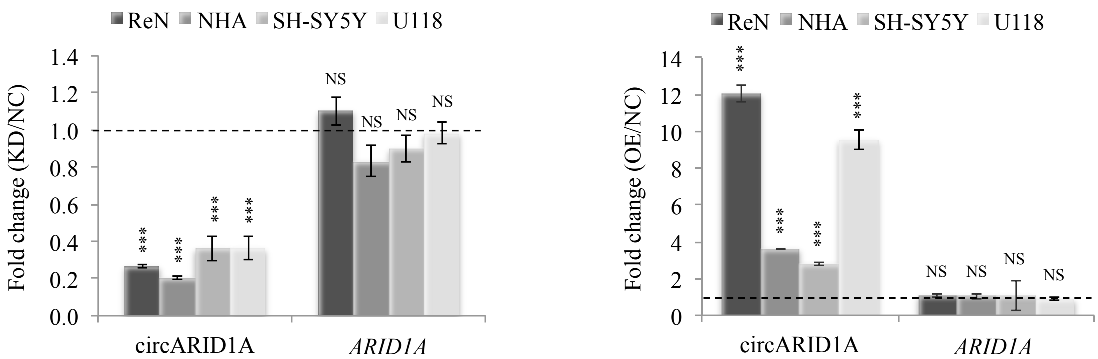

Figure 27. qRT-PCR analyses of the expression of circARID1A and *ARID1A* after circARID1A knockdown or overexpression in various neuronal cell lines.

NC, negative control. KD, knockdown. OE, overexpression.

doi:10.6342/NTU202000765

Notably, miR-204-3p expression significantly increased and decreased after knockdown and overexpression of circARID1A, respectively (Fig. 28). We hypothesized that circARID1A may serve as a sponge for miR-204-3p.

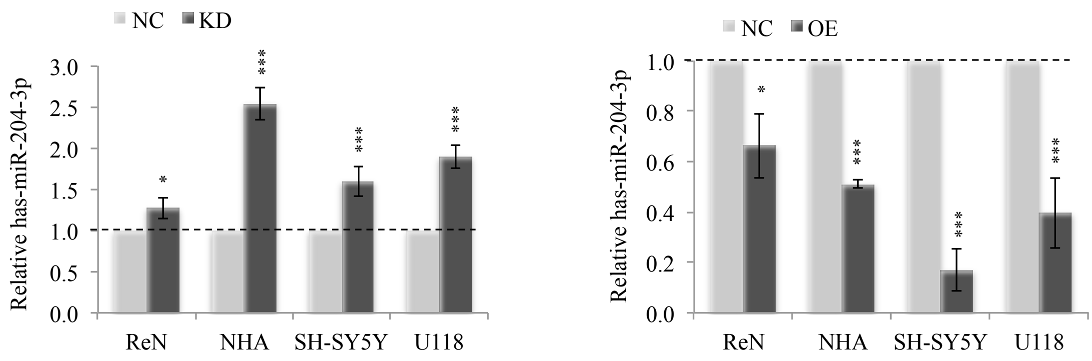

Figure 28. qRT-PCR analyses of the correlations between the expression of circARID1A and miR-204-3p after circARID1A knockdown or overexpression in various human neuronal cell lines.

To verify our prediction, luciferase reporter assay was performed to confirm the relationship between circARID1A and miR-204-3p. Various human neuronal cell lines were co-transfected the Gluc-circARID1A reporter, together with either miR-204-3p mimic or scramble mimic. Dual-luciferase activity of GLuc-circARID1A showed that miR-204-3p significantly reduced the luciferase activity as compared with scramble control (Fig. 29).

doi:10.6342/NTU202000765

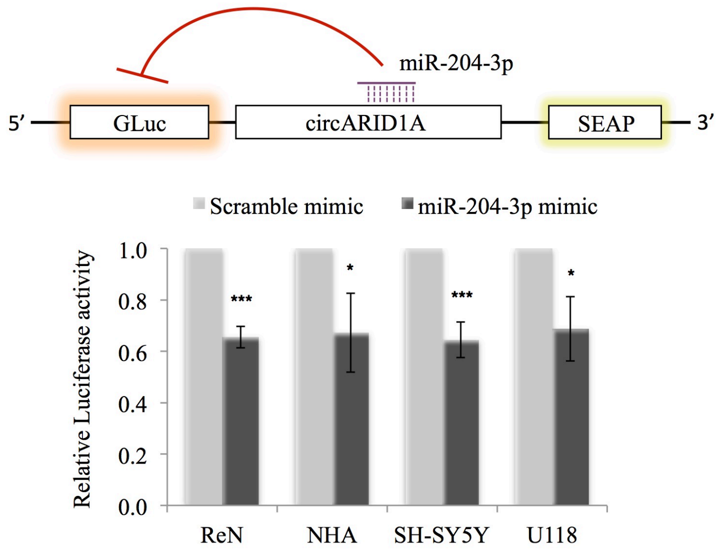

Figure 29. Luciferase reporter assay for the interaction between circARID1A and miR-204-3p.

To further examine the specificity of the binding between circARID1A and miR-204-3p, We also mutated miR-204-3p binding sites from the luciferase reporter (Fig. 30A) and found that transfection of miR-204-3p had no significant effect on the luciferase activity of the GLuc-circARID1A mutated reporter as compared to the scrambled negative control (Fig. 30B). These results thus confirmed the regulatory role of circARID1A as a miR-204-3p sponge.

doi:10.6342/NTU202000765

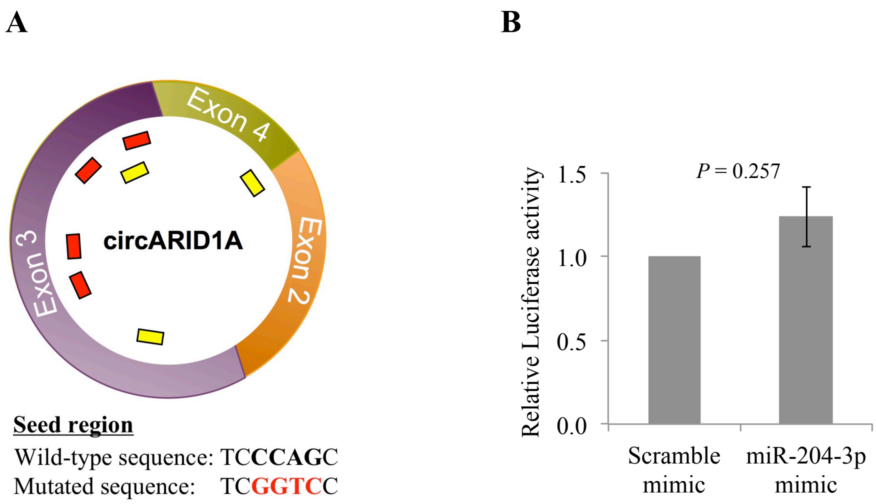

Figure 30. Site-directed mutagenesis of the potential binding sites of miR-204-3p in GLuc-circARID1A reporter construct.

(A) Schematic illustration of mutated putative miR-204-3p binding sites in luciferase reporter vectors labeled by red. (B) Luciferase assays of the NHA cells co-transfected with mutated reporter mimics.

In addition, we also showed that miR-204-3p overexpression did not significantly affect circARID1A expression (Fig. 31). These results thus confirmed the negative regulation between circARID1A and miR-204-3p and the regulatory role of circARID1A in the miR-204-3p sponge.

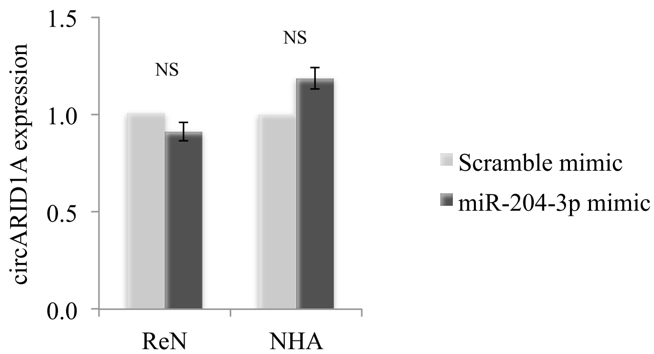

Figure 31. The expression level of circARID1A after overexpression of miR-204-3p in ReN and NHA cells.

P values are determined using two-tailed *t*-test.

doi:10.6342/NTU202000765

3.6 Regulation of ASD risk genes via the identified circRNA–miRNA interaction

We have shown that circARID1A can function as a sponge to miR-204-3p, and 171 predicted downstream targets were interacted with circARID1A–miR-204-3p axes (Fig. 32A). Identification of the predicted expression change of 171 target genes (including 12 ASD risk genes) by circARID1A and miR-204-3p. We performed circARID1A knockdown, circARID1A overexpression, and miR-204-3p overexpression in ReNcell, respectively (Fig. 32B). Then examined the fold changes of the target gene expression by microarray analysis.

The microarray raw data have been uploaded on the NCBI Gene Expression Omnibus (GEO; https://www.ncbi.nlm.nih.gov/geo/) under accession number GSE145417. All microarray analysis results, identified circRNA-miRNA-mRNA axes and the codes used in this study were uploaded on Github (https://github.com/TreesLab/circRNA_ASD). Of note, the coordinates used in this study are 1-based.

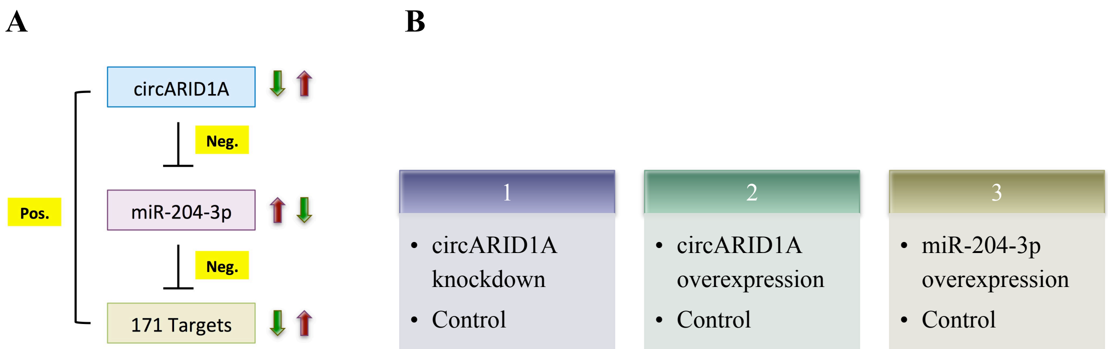

Figure 32. Examination of predicted target gene expression after perturbed circARID1A and miR-204-3p using microarray analyses.

(A) Schematic diagram representing the circARID1A–miR-204-3p regulatory pathway and its regulated targets. (B) Microarray experiments of six conditions in ReNcell.

Regarding 171 target genes, fold changes after circARID1A knockdown were indeed significantly positively correlated with those after miR-204-3p overexpression (Fig. 33A). In contract, negative correlation between gene fold changes after circARID1A

doi:10.6342/NTU202000765

overexpression and circARID1A knockdown (Fig. 33B) or circARID1A overexpression and miR-204-3p overexpression (Fig. 33C). These results were consistent with our bioinformatics predictions.

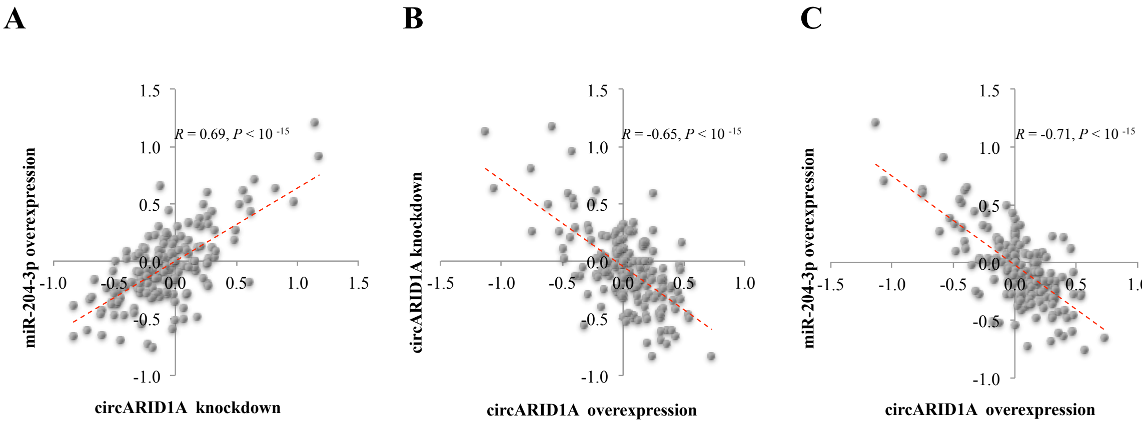

Figure 33. The correlations between $\log_2$ (fold change) of target genes expression after knockdown circARID1A, overexpress circARID1A, and overexpress miR-204-3p.

The Pearson's correlation coefficient (*R*) and *P* value are shown.

As expected, target genes with the treatment of circARID1A overexpression exhibited significant upregulation as compared to those with circARID1A knockdown and those with miR-204-3p overexpression (both *P* values are determined by one-tailed paired *t*-test), whereas there was no significant difference between the mRNA fold changes after circARID1A knockdown and those after miR-204-3p overexpression (*P* values are determined by two-tailed paired *t*-test) (Fig. 34).

doi:10.6342/NTU202000765

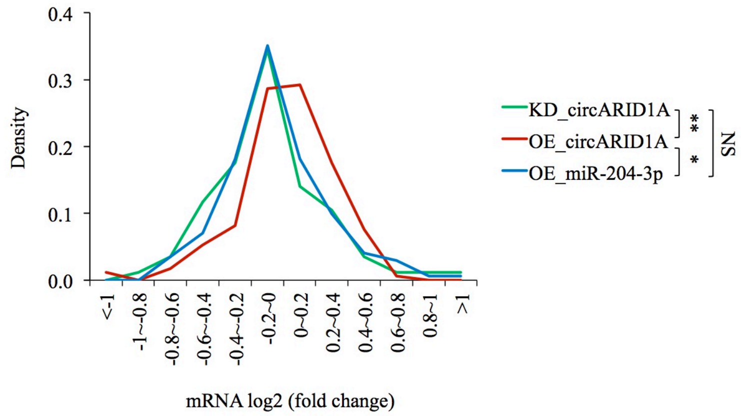

Figure 34. Distribution of the target mRNA $\log_2$ (fold change) in response to knockdown of circARID1A, overexpression of circARID1A, and overexpression of miR-204-3p.

The 171 genes included 12 ASD risk genes, 2 FMRP targets[194], 102 HuR targets[195], and 5 RBFOX1 targets[196]. For the 12 ASD risk genes, 8 genes were also HuR targets. CircARID1A overexpression led a pronounced increase for 12 ASD risk genes, whereas the reverse was observed for circARID1A knockdown or miR-204-3p overexpression in ReNcell (Fig. 35). These results were consistent with our speculation.

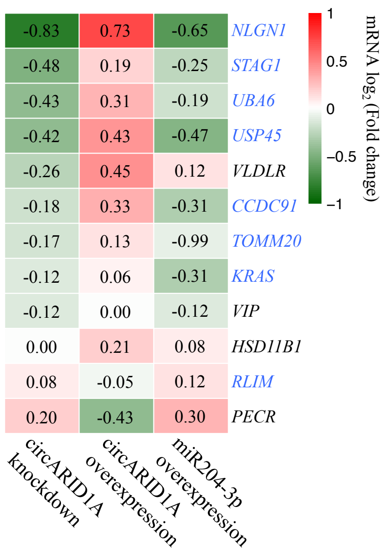

Figure 35. Heat map of the 12 ASD risk mRNA expression in response to knockdown of circARID1A, overexpression of circARID1A, and overexpression of miR-204-3p, respectively.

doi:10.6342/NTU202000765

The gene symbols highlighted in blue represent that the genes are also HuR targets.

To further test whether the circARID1A–miR-204-3p axis can regulate genes implicated in ASD, we selected the 12 ASD risk genes and experimentally examined the regulatory interactions between the axis and the ASD risk genes in ReN and NHA cells, respectively. We found that the four SFARI genes (*NLGN1, STAG1, UBA6, HSD11B1, VIP*) were significantly downregulated by knockdown of circARID1A and the overexpression of miR-204-3p, respectively. The miR-204-3p-mediated repression of the five SFARI genes was rescued by ectopic expression of circARID1A (Fig. 36). Taken together, these results suggest that circARID1A could regulate some ASD risk genes by directly sponging miR-204-3p. Our results thus suggest that circRNAs can function as efficient miRNA sponges for downstream regulation of the corresponding ASD risk genes.

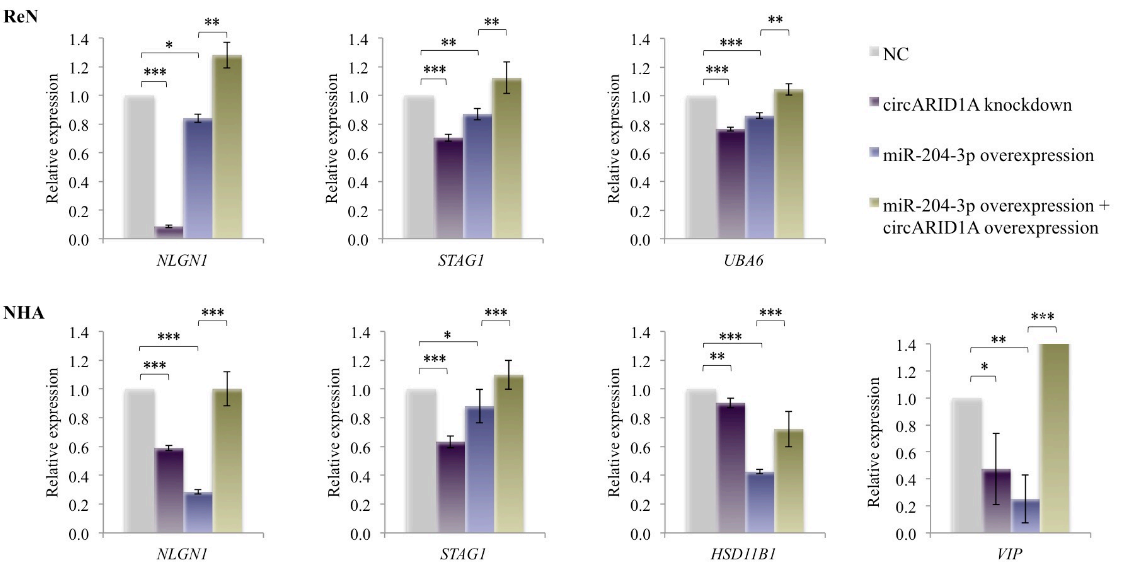

Figure 36. qRT-PCR analyses of ASD risk gene expression in ReNc (top) and NHA (bottom) cells after circARID1A knockdown, miR-204-3p overexpression, and miR-204-3p overexpression with circARID1A overexpression, respectively.

NC, negative control. *P* values are determined by two-tailed *t*-test.

doi:10.6342/NTU202000765

Furthermore, we differentiated ReNcell into different neural cell types. Undifferentiated ReNcell has visible proliferation markers MKI67. Following 14 days of differentiation, βIII-tubulin-positive neuronal cells and GFAP-positive glial cells were observed in the differentiated ReNcell (Fig. 37).

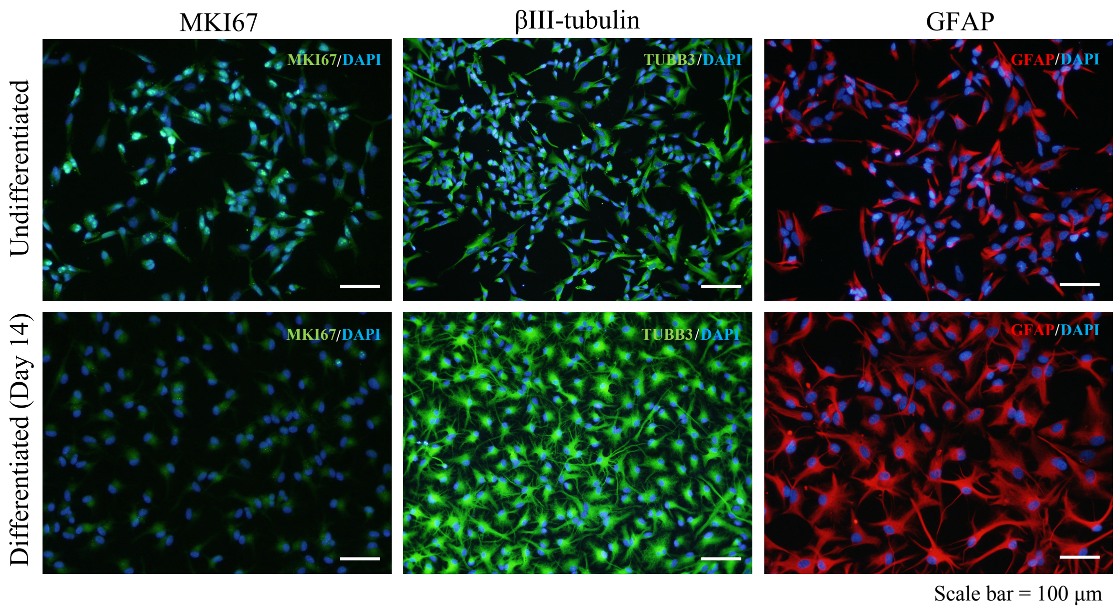

Figure 37. Fluorescent imaging of ReNcell differentiated for 14 days.

Immunostaining for undifferentiated (top) and differentiated (bottom) ReNcell with the proliferation marker MKI67 (green), the neuronal marker βIII-tubulin (green), and the mature glial cell marker GFAP (red). Nuclei are stained with DAPI (blue). Scale bar, 100 μm.

We found that circARID1A expression was significantly positively correlated with the expression of *NLGN1* and *STAG1* during ReNcell differentiation (Fig. 38). Of note, both *NLGN1* and *STAG1* were also HuR targets, which were demonstrated to be associated with neurodevelopmental defects[197], alteration of expression of HuR targets may contribute to the developing neocortex and then in autism pathogenesis[198]. Taken

doi:10.6342/NTU202000765

together, these results revealed that circARID1A could regulate genes implicated in ASD through directly sponging miR-204-3p.

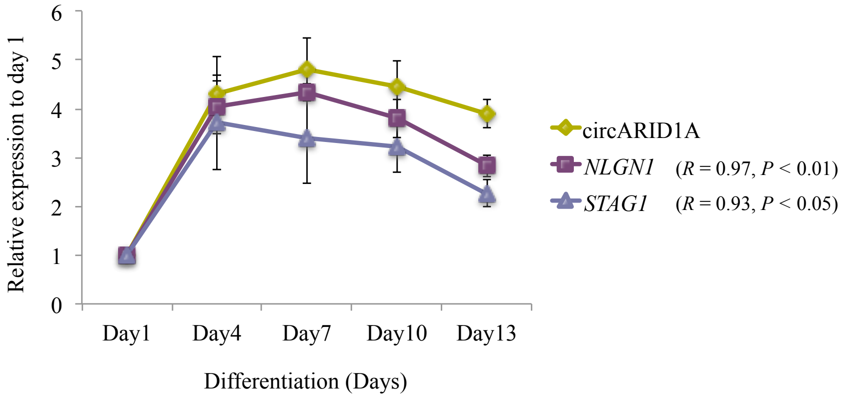

Figure 38. Relative expression of circARID1A and two ASD risk genes (*NLGN1* and *STAG1*) during ReNcell differentiation.

The Pearson correlation coefficients (R) between the expression of circARID1A and the two ASD risk genes and *P* values are shown in parentheses.

doi:10.6342/NTU202000765

CHAPTER 4. Discussion

We systematically investigate circRNA dysregulation in ASD cortex and constructed the corresponding ASD-associated circRNA–miRNA–mRNA regulatory networks. Like the previous observations for mRNAs[8,78], miRNAs[12] and circRNAs[96] in ASD, our PCA result for circRNA expression profiles also revealed that frontal cortex and temporal cortex samples clustered together but cortex and cerebellar vermis samples grouped into separate clusters (Fig. 7). We also showed that the fold changes for the DE-circRNAs were concordant between the FC and TC, and were not biased by a small number of samples with removal of dup15q, low RIN, or high PMI (Fig. 10). While ASD and non-ASD samples can be grouped into two separate clusters based on the 60 identified DE-circRNAs by both PCA (Fig. 11) and hierarchical clustering (Fig. 12) analyses, but did not show separate clustering based on their host genes expression profiles. We thus provided a shared circRNA dysregulation signature among the majority of ASD samples.

In this study, we investigated genome-wide circRNA expression in ASD cortex samples and the corresponding ASD-associated circRNA–miRNA–mRNA axes. Regarding the identified ASD-associated circRNAs and the previously identified DE-miRNAs derived from the same cortex samples used in this study, we thus constructed 8,170 ASD-associated circRNA–miRNA–mRNA interactions (Fig. 17). Notably, within the 2,302 target genes of ASD-associated interactions, we observed significant enrichment for ASD risk genes, but not for genes implicated in monogenetic forms of other brain

doi:10.6342/NTU202000765

disorders. Such as epilepsy, which is often a comorbidity of ASD. Regarding a recently published dataset of 102 high-confidence ASD genetic risk genes[68], the 2,302 target genes also exhibited significant enrichment for the high-confidence ASD genetic risk genes (Fig. 39).

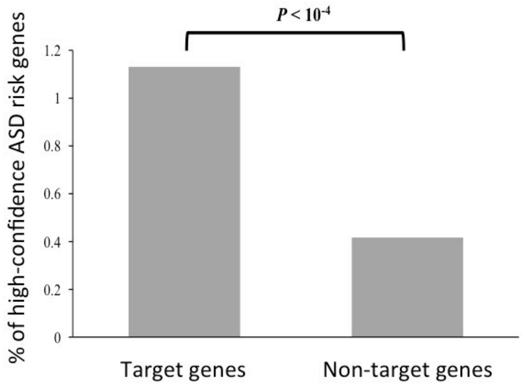

Figure 39. Enrichment of high-confidence ASD risk genes for the targets of the identified circRNA–miRNA–mRNA interactions.

The high-confidence ASD genetic risk factors were derived from whole-exome sequencing on 35,584 ASD subjects. The *P* value is determined by two-tailed Fisher's exact test.

Moreover, we observed that target genes of the ASD-associated circRNA–miRNA–mRNA axes were significantly enriched in genes encoding inhibitory PSD proteins, but not in those encoding excitatory PSD ones (Fig. 19A). This result reflects the previous reports that there is an E/I neuronal imbalance in ASD and that inhibitory neurons are overproduced in ASD patient-derived organoids[77,185,193]. These results suggest that the identified ASD-associated circRNA–miRNA axes may serve as an alternative pathway to perturb key transcript levels and thereby contribute to ASD susceptibility.

doi:10.6342/NTU202000765

On the basis of the hypothesis of circRNAs serve as microRNA sponge, we utilized differential expressed circRNA, miRNA and mRNA profiles of the ASD patients combined with experimentally validated miRNA–target interactions to reconstruct circRNA-associated network for the progression of ASD. However, the identified ASD-associated circRNA–miRNA–mRNA networks are constructed based on the correlation analysis and bioinformatics prediction, which need extensive experimental validation to investigate the interactions. As our experimental validation of circARID1A, we further characterized and functionally evaluated the circARID1A–miR-204-3p axis. Notable, we confirmed that the expressions of five SFARI genes (*NLGN1, STAG1, HSD11B1, VIP and UBA6*) were regulated by circARID1A via sponging miR-204-3p (Fig. 36).

The expression of both *NLGN1* and *STAG1* exhibited a significantly positive correlation with the circARID1A expression during ReNcell differentiation (Fig. 38). Recent evidence suggests that NLGN1 play an important role in a variety of activity-dependent response[97] and memory formation[98-100]. Knockout of NLGN1 could cause increased repetitive behavior[100], and with mutation in NLGN1 could cause abnormal social behavior in mouse models[199]. Alteration of NLGN1 expression in specific excitatory and inhibitory neuronal subpopulations can affect the dynamic processes of memory consolidation and strengthening[98]. Therefore, the identified circARID1A–miR-204-3p axis, which regulates *NLGN1* expression, may provide a useful molecular mechanism of excitation and inhibition underlying long-term memory consolidation and strengthening for further developing potential therapeutic strategies to address these neuropsychiatric disorders, including ASD. Previous study has showed a higher proportion of inhibitory

doi:10.6342/NTU202000765

neurons than excitatory neurons in ASD[193]. Also, ASD-associated genes were reported to be especially enriched in inhibitory neurons[185]. Afterward, we can differentiate ReNcell and then examine if knockdown or overexpression circARID1A alters the balance between inhibitory and excitatory neuron.

In addition, VIP and UBA6 have been demonstrated to play an essential regulatory role during rodent embryonic development[101,102]. VIP is known as a regulator of embryogenesis of neural tube closure; interference with VIP can result in permanent effects on adult social behavior[102]. It was shown that UBA6 brain-specific knockout mice exhibited social impairment and reduced vocalizations, representing a valid ASD mouse model[103]. As a regulator of multiple ASD-associated genes, the circARID1A–miR-204-3p axis would be a valuable candidate for further ASD pathophysiology study.

In summary, our study provides a global view of circRNAs in ASD and non-ASD cortex. By integrating ASD candidate gene sets, miRNA and circRNA dysregulation data derived from the same ASD cortex samples, we have explored multiple lines of evidence for the functional role of ASD for circRNA dysregulation and the corresponding circRNA–miRNA–mRNA networks. That may lead to improve ASD diagnosis and treatment in the future.

doi:10.6342/NTU202000765

CHAPTER 5. Future works

Increasing evidence shows that circRNAs play an important role in many diseases. CircRNAs with more stable structure than linear RNAs in peripheral blood[200] and body fluids[201], which could be use as biomarkers of diseases and thus improve the accuracy and specificity of diagnosis[202]. However, the regulation of their biogenesis and degradation remains largely unclear. CircRNAs may be eliminated from cells by siRNAs[87], microvesicles or exosomes[203,204]. Whether circARID1A is degraded by the similar mechanism still needs further exploration.

It is noteworthy that circARID1A was validated to be widely expressed in the brain of multiple vertebrate species from human to chicken (Fig. 23), suggesting the evolutionary importance of this circRNA across vertebrate species. This observation also implies a possibility that future studies may further examine whether circARID1A serves as an early pathogenic feature during neurodevelopmental processes by altering circARID1A expression in appropriate transgenic animal models such as mice. In addition, we observed circARID1A was highly expressed in multiple brain regions. This raises an interesting question of whether circARID1A dysregulation could occur in multiple cell types or cell composition in ASD brains.

Moreover, a study mentioned that transfection of miRNA mimics may led to the accumulation of high molecular weight RNA species[205], and a few hundred fold increase in mature miRNA levels may occupied too many RNA-induced silencing complexes (RISCs) then affect the function of the other endogenous miRNA-target pool.

doi:10.6342/NTU202000765

Therefore, in the future study, we could use lentiviral transduction, plasmid transfection and transgenic expression of miRNAs to avoid RNA accumulation in cells.

On the other hand, the genetic architecture of autism has proved to be complex and heterogeneous, however recent research revealed that ASD and cancer might share common genetic architecture[206]. For example, colorectal and breast cancer-associated genes highly (~30%) overlapping with ASD[206], particularly those involved in cell-signaling pathways such as MAPK and calcium signaling[207]. circARID1A upregulated in ASD cortex, and also upregulated more than 6-fold in chemoradiation-resistant colorectal cancer[208], which imply that circARID1A may also play a potential role in colorectal cancer. The host gene of circARID1A can regulate transcription of certain gene by altering the chromatin remodeling, which serve as a tumor suppressor and has been generally found mutated in different type of cancers[209-211].

CircRNAs can act as a sponge by trapping miRNAs. However, most of circRNAs do not contain a great number of binding sites for a particular miRNA. Recent studies showed that circRNAs may not require multiple binding sites to function like miRNA sponge, such as circHIPK3[88], circCCDC66[132] and circTP63[133]. In other words, circRNAs might be associated with a variety of miRNAs. As our prediction by RNA22, circARID1A has 21 binding sites of 7 DE-miRNAs. Consequently, disturbing a circRNA expression may affect more than one miRNA, and affect the expression of a larger number of miRNA targets. Meanwhile, some miRNAs mediated by several circRNAs.

doi:10.6342/NTU202000765

CircRNAs not only serve as miRNA sponges, but also act as protein sponges by binding RBPs. Moreover, some circRNAs also contain internal ribosome entry site (IRES) can directly translate peptides. We hope to explore the effect of circRNAs in ASD pathophysiology from other directions in the future.

doi:10.6342/NTU202000765

CHAPTER 6. Reference

1 Yasui, D. H. *et al.* 15q11.2-13.3 chromatin analysis reveals epigenetic regulation of CHRNA7 with deficiencies in Rett and autism brain. *Hum Mol Genet* **20**, 4311-4323, doi:10.1093/hmg/ddr357 (2011).

2 Lyall, K. *et al.* The Changing Epidemiology of Autism Spectrum Disorders. *Annu Rev Public Health* **38**, 81-102, doi:10.1146/annurev-publhealth-031816-044318 (2017).

3 Siu, M. T. & Weksberg, R. Epigenetics of Autism Spectrum Disorder. *Adv Exp Med Biol* **978**, 63-90, doi:10.1007/978-3-319-53889-1_4 (2017).

4 Frazier, T. W. *et al.* Validation of proposed DSM-5 criteria for autism spectrum disorder. *J Am Acad Child Adolesc Psychiatry* **51**, 28-40 e23, doi:10.1016/j.jaac.2011.09.021 (2012).

5 Saemundsen, E., Magnusson, P., Georgsdottir, I., Egilsson, E. & Rafnsson, V. Prevalence of autism spectrum disorders in an Icelandic birth cohort. *BMJ Open* **3**, doi:10.1136/bmjopen-2013-002748 (2013).

6 Kim, Y. S. *et al.* Prevalence of autism spectrum disorders in a total population sample. *Am J Psychiatry* **168**, 904-912, doi:10.1176/appi.ajp.2011.10101532 (2011).

7 Blumberg, S. J. *et al.* Changes in prevalence of parent-reported autism spectrum disorder in school-aged U.S. children: 2007 to 2011-2012. *Natl Health Stat Report*, 1-11, 11 p following 11 (2013).

8 Lord, C. & Bishop, S. L. Recent Advances in Autism Research as Reflected in DSM-5 Criteria for Autism Spectrum Disorder. *Annu Rev Clin Psycho* **11**, 53-70, doi:10.1146/annurev-clinpsy-032814-112745 (2015).

9 Sztainberg, Y. & Zoghbi, H. Y. Lessons learned from studying syndromic autism spectrum disorders. *Nat Neurosci* **19**, 1408-1417, doi:10.1038/nn.4420 (2016).

10 Lord, C. & Jones, R. M. Annual Research Review: Re-thinking the classification of autism spectrum disorders. *J Child Psychol Psyc* **53**, 490-509, doi:10.1111/j.1469-7610.2012.02547.x (2012).

11 Chen, R., Jiao, Y. & Herskovits, E. H. Structural MRI in autism spectrum disorder. *Pediatr Res* **69**, 63R-68R, doi:10.1203/PDR.0b013e318212c2b3 (2011).

12 Wegiel, J. *et al.* Stereological study of the neuronal number and volume of 38 brain subdivisions of subjects diagnosed with autism reveals significant alterations restricted to the striatum, amygdala and cerebellum. *Acta Neuropathol Commun* **2**, 141, doi:10.1186/s40478-014-0141-7 (2014).

13 van Kooten, I. A. *et al.* Neurons in the fusiform gyrus are fewer and smaller in autism. *Brain* **131**, 987-999, doi:10.1093/brain/awn033 (2008).

14 Courchesne, E. *et al.* Neuron Number and Size in Prefrontal Cortex of Children With Autism. *Jama-J Am Med Assoc* **306**, 2001-2010, doi:10.1001/jama.2011.1638 (2011).

doi:10.6342/NTU202000765

15 Voineagu, I. *et al.* Transcriptomic analysis of autistic brain reveals convergent molecular pathology. *Nature* **474**, 380-384, doi:10.1038/nature10110 (2011).
16 Parikshak, N. N. *et al.* Genome-wide changes in lncRNA, splicing, and regional gene expression patterns in autism. *Nature* **540**, 423-427, doi:10.1038/nature20612 (2016).
17 Dichter, G. S. Functional magnetic resonance imaging of autism spectrum disorders. *Dialogues Clin Neurosci* **14**, 319-351 (2012).
18 Philip, R. C. *et al.* A systematic review and meta-analysis of the fMRI investigation of autism spectrum disorders. *Neurosci Biobehav Rev* **36**, 901-942, doi:10.1016/j.neubiorev.2011.10.008 (2012).
19 Pelphrey, K. A., Shultz, S., Hudac, C. M. & Vander Wyk, B. C. Research review: Constraining heterogeneity: the social brain and its development in autism spectrum disorder. *J Child Psychol Psychiatry* **52**, 631-644, doi:10.1111/j.1469-7610.2010.02349.x (2011).
20 Supekar, K. *et al.* Brain Hyperconnectivity in Children with Autism and its Links to Social Deficits. *Cell Rep* **5**, 738-747, doi:10.1016/j.celrep.2013.10.001 (2013).
21 Belmonte, M. K. *et al.* Autism and abnormal development of brain connectivity. *J Neurosci* **24**, 9228-9231, doi:10.1523/JNEUROSCI.3340-04.2004 (2004).
22 Minshew, N. J. & Keller, T. A. The nature of brain dysfunction in autism: functional brain imaging studies. *Curr Opin Neurol* **23**, 124-130, doi:10.1097/WCO.0b013e32833782d4 (2010).
23 Just, M. A., Keller, T. A., Malave, V. L., Kana, R. K. & Varma, S. Autism as a neural systems disorder: A theory of frontal-posterior underconnectivity. *Neurosci Biobehav R* **36**, 1292-1313, doi:10.1016/j.neubiorev.2012.02.007 (2012).
24 Lai, M. C., Lombardo, M. V. & Baron-Cohen, S. Autism. *Lancet* **383**, 896-910, doi:10.1016/S0140-6736(13)61539-1 (2014).
25 Croen, L. A. *et al.* The health status of adults on the autism spectrum. *Autism* **19**, 814-823, doi:10.1177/1362361315577517 (2015).
26 Sala, G., Hooley, M., Attwood, T., Mesibov, G. B. & Stokes, M. A. Autism and Intellectual Disability: A Systematic Review of Sexuality and Relationship Education. *Sex Disabil* **37**, 353-382, doi:10.1007/s11195-019-09577-4 (2019).
27 Crane, L., Goddard, L. & Pring, L. Sensory processing in adults with autism spectrum disorders. *Autism* **13**, 215-228, doi:10.1177/1362361309103794 (2009).
28 Ben-Sasson, A. *et al.* A meta-analysis of sensory modulation symptoms in individuals with autism spectrum disorders. *J Autism Dev Disord* **39**, 1-11, doi:10.1007/s10803-008-0593-3 (2009).
29 Simonoff, E. *et al.* Psychiatric disorders in children with autism spectrum disorders: prevalence, comorbidity, and associated factors in a population-derived sample. *J Am Acad Child Adolesc Psychiatry* **47**, 921-929, doi:10.1097/CHI.0b013e318179964f (2008).
30 Lugo-Marin, J. *et al.* Prevalence of psychiatric disorders in adults with autism spectrum disorder: A systematic review and meta-analysis. *Res Autism Spect Dis* **59**, 22-33, doi:10.1016/j.rasd.2018.12.004 (2019).

doi:10.6342/NTU202000765

31 Bolton, P. F. *et al.* Epilepsy in autism: features and correlates. *Br J Psychiatry* **198**, 289-294, doi:10.1192/bjp.bp.109.076877 (2011).

32 Chaidez, V., Hansen, R. L. & Hertz-Picciotto, I. Gastrointestinal problems in children with autism, developmental delays or typical development. *J Autism Dev Disord* **44**, 1117-1127, doi:10.1007/s10803-013-1973-x (2014).

33 Comi, A. M., Zimmerman, A. W., Frye, V. H., Law, P. A. & Peeden, J. N. Familial clustering of autoimmune disorders and evaluation of medical risk factors in autism. *J Child Neurol* **14**, 388-394, doi:Doi 10.1177/088307389901400608 (1999).

34 Souders, M. C. *et al.* Sleep in Children with Autism Spectrum Disorder. *Curr Psychiatry Rep* **19**, 34, doi:10.1007/s11920-017-0782-x (2017).

35 Kent, R. & Simonoff, E. in *Anxiety in children and adolescents with autism spectrum disorder* 5-32 (Elsevier, 2017).

36 Hollocks, M. J., Lerh, J. W., Magiati, I., Meiser-Stedman, R. & Brugha, T. S. Anxiety and depression in adults with autism spectrum disorder: a systematic review and meta-analysis. *Psychol Med* **49**, 559-572, doi:10.1017/S0033291718002283 (2019).

37 Sanders, S. J. *et al.* De novo mutations revealed by whole-exome sequencing are strongly associated with autism. *Nature* **485**, 237-241, doi:10.1038/nature10945 (2012).

38 Sebat, J. *et al.* Strong association of de novo copy number mutations with autism. *Science* **316**, 445-449, doi:10.1126/science.1138659 (2007).

39 Pinto, D. *et al.* Functional impact of global rare copy number variation in autism spectrum disorders. *Nature* **466**, 368-372, doi:10.1038/nature09146 (2010).

40 Glessner, J. T. *et al.* Autism genome-wide copy number variation reveals ubiquitin and neuronal genes. *Nature* **459**, 569-573, doi:10.1038/nature07953 (2009).

41 Tordjman, S. *et al.* Gene x environment interactions in autism spectrum disorders: role of epigenetic mechanisms. *Front Psychiatry* **5**, doi:10.3389/fpsyt.2014.00053 (2014).

42 Hultman, C. M., Sandin, S., Levine, S. Z., Lichtenstein, P. & Reichenberg, A. Advancing paternal age and risk of autism: new evidence from a population-based study and a meta-analysis of epidemiological studies. *Mol Psychiatry* **16**, 1203-1212, doi:10.1038/mp.2010.121 (2011).

43 Lampi, K. M. *et al.* Parental age and risk of autism spectrum disorders in a Finnish national birth cohort. *J Autism Dev Disord* **43**, 2526-2535, doi:10.1007/s10803-013-1801-3 (2013).

44 Wang, M. Y., Li, K. Q., Zhao, D. M. & Li, L. The association between maternal use of folic acid supplements during pregnancy and risk of autism spectrum disorders in children: a meta-analysis. *Mol Autism* **8**, doi:10.1186/s13229-017-0170-8 (2017).

45 Rai, D. *et al.* Parental depression, maternal antidepressant use during pregnancy, and risk of autism spectrum disorders: population based case-control study. *Bmj-Brit Med J* **346**, doi:10.1136/bmj.f2059 (2013).

doi:10.6342/NTU202000765

46 Bai, D. *et al.* Association of Genetic and Environmental Factors With Autism in a 5-Country Cohort. *JAMA Psychiatry*, doi:10.1001/jamapsychiatry.2019.1411 (2019).
47 Ronald, A. & Hoekstra, R. A. Autism spectrum disorders and autistic traits: a decade of new twin studies. *Am J Med Genet B Neuropsychiatr Genet* **156B**, 255-274, doi:10.1002/ajmg.b.31159 (2011).
48 Abrahams, B. S. & Geschwind, D. H. Advances in autism genetics: on the threshold of a new neurobiology. *Nat Rev Genet* **9**, 341-355, doi:10.1038/nrg2346 (2008).
49 Hallmayer, J. *et al.* Genetic Heritability and Shared Environmental Factors Among Twin Pairs With Autism. *Arch Gen Psychiat* **68**, 1095-1102, doi:10.1001/archgenpsychiatry.2011.76 (2011).
50 Mody, M. & Belliveau, J. W. Speech and Language Impairments in Autism: Insights from Behavior and Neuroimaging. *N Am J Med Sci (Boston)* **5**, 157-161, doi:10.7156/v5i3p157 (2013).
51 Hansen, S. N. *et al.* Recurrence Risk of Autism in Siblings and Cousins: A Multinational, Population-Based Study. *J Am Acad Child Adolesc Psychiatry* **58**, 866-875, doi:10.1016/j.jaac.2018.11.017 (2019).
52 Gronborg, T. K., Schendel, D. E. & Parner, E. T. Recurrence of autism spectrum disorders in full- and half-siblings and trends over time: a population-based cohort study. *JAMA Pediatr* **167**, 947-953, doi:10.1001/jamapediatrics.2013.2259 (2013).
53 Ozonoff, S. *et al.* Recurrence Risk for Autism Spectrum Disorders: A Baby Siblings Research Consortium Study. *Pediatrics* **128**, E488-E495, doi:10.1542/peds.2010-2825 (2011).
54 Won, H., Mah, W. & Kim, E. Autism spectrum disorder causes, mechanisms, and treatments: focus on neuronal synapses. *Front Mol Neurosci* **6**, 19, doi:10.3389/fnmol.2013.00019 (2013).
55 Chen, J. A., Penagarikano, O., Belgard, T. G., Swarup, V. & Geschwind, D. H. The emerging picture of autism spectrum disorder: genetics and pathology. *Annu Rev Pathol* **10**, 111-144, doi:10.1146/annurev-pathol-012414-040405 (2015).
56 Wang, Z. J. *et al.* Correction: Amelioration of autism-like social deficits by targeting histone methyltransferases EHMT1/2 in Shank3-deficient mice. *Mol Psychiatry*, doi:10.1038/s41380-019-0524-z (2019).
57 Berryer, M. H. *et al.* Mutations in SYNGAP1 cause intellectual disability, autism, and a specific form of epilepsy by inducing haploinsufficiency. *Hum Mutat* **34**, 385-394, doi:10.1002/humu.22248 (2013).
58 Strauss, K. A. *et al.* Recessive symptomatic focal epilepsy and mutant contactin-associated protein-like 2. *N Engl J Med* **354**, 1370-1377, doi:10.1056/NEJMoa052773 (2006).
59 Harris, S. W. *et al.* Autism profiles of males with fragile X syndrome. *Am J Ment Retard* **113**, 427-438, doi:10.1352/2008.113:427-438 (2008).
60 Chao, H. T. *et al.* Dysfunction in GABA signalling mediates autism-like stereotypies and Rett syndrome phenotypes. *Nature* **468**, 263-269, doi:10.1038/nature09582 (2010).

doi:10.6342/NTU202000765

61 Guan, J. *et al.* Exploiting aberrant mRNA expression in autism for gene discovery and diagnosis. *Hum. Genet.* **135**, 797-811 (2016).
62 Irimia, M. *et al.* A highly conserved program of neuronal microexons is misregulated in autistic brains. *Cell* **159**, 1511-1523, doi:10.1016/j.cell.2014.11.035 (2014).
63 Wang, Y. *et al.* Genome-wide differential expression of synaptic long noncoding RNAs in autism spectrum disorder. *Transl Psychiatry* **5**, e660, doi:10.1038/tp.2015.144 (2015).
64 Wu, Y. E., Parikshak, N. N., Belgard, T. G. & Geschwind, D. H. Genome-wide, integrative analysis implicates microRNA dysregulation in autism spectrum disorder. *Nat Neurosci* **19**, 1463-1476, doi:10.1038/nn.4373 (2016).
65 Ander, B. P., Barger, N., Stamova, B., Sharp, F. R. & Schumann, C. M. Atypical miRNA expression in temporal cortex associated with dysregulation of immune, cell cycle, and other pathways in autism spectrum disorders. *Mol Autism* **6**, 37, doi:10.1186/s13229-015-0029-9 (2015).
66 Vogel Ciernia, A. & LaSalle, J. The landscape of DNA methylation amid a perfect storm of autism aetiologies. *Nat Rev Neurosci* **17**, 411-423, doi:10.1038/nrn.2016.41 (2016).
67 Shulha, H. P. *et al.* Epigenetic signatures of autism: trimethylated H3K4 landscapes in prefrontal neurons. *Archives of general psychiatry* **69**, 314-324, doi:10.1001/archgenpsychiatry.2011.151 (2012).
68 Sun, W. *et al.* Histone Acetylome-wide Association Study of Autism Spectrum Disorder. *Cell* **167**, 1385-1397 e1311, doi:10.1016/j.cell.2016.10.031 (2016).
69 Berg, J. M. & Geschwind, D. H. Autism genetics: searching for specificity and convergence. *Genome Biol* **13**, 247, doi:10.1186/gb4034 (2012).
70 Bourgeron, T. From the genetic architecture to synaptic plasticity in autism spectrum disorder. *Nat Rev Neurosci* **16**, 551-563, doi:10.1038/nrn3992 (2015).
71 RK, C. Y. *et al.* Whole genome sequencing resource identifies 18 new candidate genes for autism spectrum disorder. *Nat Neurosci* **20**, 602-611, doi:10.1038/nn.4524 (2017).
72 Betancur, C., Sakurai, T. & Buxbaum, J. D. The emerging role of synaptic cell-adhesion pathways in the pathogenesis of autism spectrum disorders. *Trends Neurosci* **32**, 402-412, doi:10.1016/j.tins.2009.04.003 (2009).
73 Stewart, L. T. Cell adhesion proteins and the pathogenesis of autism spectrum disorders. *J Neurophysiol* **113**, 1283-1286, doi:10.1152/jn.00780.2013 (2015).
74 Gupta, S. *et al.* Transcriptome analysis reveals dysregulation of innate immune response genes and neuronal activity-dependent genes in autism. *Nat Commun* **5**, 5748, doi:10.1038/ncomms6748 (2014).
75 Patel, S. *et al.* Social impairments in autism spectrum disorder are related to maternal immune history profile. *Mol Psychiatry*, doi:10.1038/mp.2017.201 (2017).
76 Casanova, M. F., Buxhoeveden, D. & Gomez, J. Disruption in the inhibitory architecture of the cell minicolumn: implications for autism. *Neuroscientist* **9**, 496-507, doi:10.1177/1073858403253552 (2003).

doi:10.6342/NTU202000765

77 Sohal, V. S. & Rubenstein, J. L. R. Excitation-inhibition balance as a framework for investigating mechanisms in neuropsychiatric disorders. *Mol Psychiatr* **24**, 1248-1257, doi:10.1038/s41380-019-0426-0 (2019).
78 Chana, G. *et al.* Decreased expression of mGluR5 within the dorsolateral prefrontal cortex in autism and increased microglial number in mGluR5 knockout mice: Pathophysiological and neurobehavioral implications. *Brain, behavior, and immunity* **49**, 197-205 (2015).
79 James, S., Shpyleva, S., Melnyk, S., Pavliv, O. & Pogribny, I. Elevated 5-hydroxymethylcytosine in the Engrailed-2 (EN-2) promoter is associated with increased gene expression and decreased MeCP2 binding in autism cerebellum. *Translational psychiatry* **4**, e460 (2014).
80 Chow, M. L. *et al.* Age-Dependent Brain Gene Expression and Copy Number Anomalies in Autism Suggest Distinct Pathological Processes at Young Versus Mature Ages. *Plos Genetics* **8**, doi:10.1371/journal.pgen.1002592 (2012).
81 Ginsberg, M. R., Rubin, R. A., Falcone, T., Ting, A. H. & Natowicz, M. R. Brain Transcriptional and Epigenetic Associations with Autism. *Plos One* **7**, doi:10.1371/journal.pone.0044736 (2012).
82 Ansel, A., Rosenzweig, J. P., Zisman, P. D., Melamed, M. & Gesundheit, B. Variation in Gene Expression in Autism Spectrum Disorders: An Extensive Review of Transcriptomic Studies. *Front Neurosci* **10**, 601, doi:10.3389/fnins.2016.00601 (2016).
83 Ashwal-Fluss, R. *et al.* circRNA biogenesis competes with pre-mRNA splicing. *Mol Cell* **56**, 55-66, doi:10.1016/j.molcel.2014.08.019 (2014).
84 Zhang, Y. *et al.* The Biogenesis of Nascent Circular RNAs. *Cell Rep* **15**, 611-624, doi:10.1016/j.celrep.2016.03.058 (2016).
85 Salzman, J., Gawad, C., Wang, P. L., Lacayo, N. & Brown, P. O. Circular RNAs are the predominant transcript isoform from hundreds of human genes in diverse cell types. *Plos One* **7**, e30733, doi:10.1371/journal.pone.0030733 (2012).
86 Memczak, S. *et al.* Circular RNAs are a large class of animal RNAs with regulatory potency. *Nature* **495**, 333-338, doi:10.1038/nature11928 (2013).
87 Jeck, W. R. *et al.* Circular RNAs are abundant, conserved, and associated with ALU repeats. *Rna* **19**, 141-157, doi:10.1261/rna.035667.112 (2013).
88 Zheng, Q. *et al.* Circular RNA profiling reveals an abundant circHIPK3 that regulates cell growth by sponging multiple miRNAs. *Nat Commun* **7**, 11215, doi:10.1038/ncomms11215 (2016).
89 Chuang, T. J. *et al.* Integrative transcriptome sequencing reveals extensive alternative trans-splicing and cis-backsplicing in human cells. *Nucleic Acids Res* **46**, 3671-3691, doi:10.1093/nar/gky032 (2018).
90 Sanger, H. L., Klotz, G., Riesner, D., Gross, H. J. & Kleinschmidt, A. K. Viroids Are Single-Stranded Covalently Closed Circular Rna Molecules Existing as Highly Base-Paired Rod-Like Structures. *P Natl Acad Sci USA* **73**, 3852-3856, doi:DOI 10.1073/pnas.73.11.3852 (1976).
91 Hsu, M. T. & Coca-Prados, M. Electron microscopic evidence for the circular form of RNA in the cytoplasm of eukaryotic cells. *Nature* **280**, 339-340, doi:10.1038/280339a0 (1979).

doi:10.6342/NTU202000765

92 Nigro, J. M. *et al.* Scrambled exons. *Cell* **64**, 607-613, doi:10.1016/0092-8674(91)90244-s (1991).
93 Li, Z. *et al.* Exon-intron circular RNAs regulate transcription in the nucleus. *Nat Struct Mol Biol* **22**, 256-264, doi:10.1038/nsmb.2959 (2015).
94 Zhang, Y. *et al.* Circular intronic long noncoding RNAs. *Mol Cell* **51**, 792-806, doi:10.1016/j.molcel.2013.08.017 (2013).
95 Liang, D. & Wilusz, J. E. Short intronic repeat sequences facilitate circular RNA production. *Genes Dev* **28**, 2233-2247, doi:10.1101/gad.251926.114 (2014).
96 Zhang, X. O. *et al.* Complementary sequence-mediated exon circularization. *Cell* **159**, 134-147, doi:10.1016/j.cell.2014.09.001 (2014).
97 Conn, S. J. *et al.* The RNA binding protein quaking regulates formation of circRNAs. *Cell* **160**, 1125-1134, doi:10.1016/j.cell.2015.02.014 (2015).
98 Kramer, M. C. *et al.* Combinatorial control of Drosophila circular RNA expression by intronic repeats, hnRNPs, and SR proteins. *Gene Dev* **29**, 2168-2182, doi:10.1101/gad.270421.115 (2015).
99 Errichelli, L. *et al.* FUS affects circular RNA expression in murine embryonic stem cell-derived motor neurons. *Nat Commun* **8**, 14741, doi:10.1038/ncomms14741 (2017).
100 Ivanov, A. *et al.* Analysis of intron sequences reveals hallmarks of circular RNA biogenesis in animals. *Cell Rep* **10**, 170-177, doi:10.1016/j.celrep.2014.12.019 (2015).
101 Wang, M., Hou, J., Muller-McNicoll, M., Chen, W. & Schuman, E. M. Long and Repeat-Rich Intronic Sequences Favor Circular RNA Formation under Conditions of Reduced Spliceosome Activity. *iScience* **20**, 237-247, doi:10.1016/j.isci.2019.08.058 (2019).
102 Liang, D. M. *et al.* The Output of Protein-Coding Genes Shifts to Circular RNAs When the Pre-mRNA Processing Machinery Is Limiting. *Mol Cell* **68**, 940-+, doi:10.1016/j.molcel.2017.10.034 (2017).
103 Rybak-Wolf, A. *et al.* Circular RNAs in the Mammalian Brain Are Highly Abundant, Conserved, and Dynamically Expressed. *Mol Cell* **58**, 870-885, doi:10.1016/j.molcel.2015.03.027 (2015).
104 Veno, M. T. *et al.* Spatio-temporal regulation of circular RNA expression during porcine embryonic brain development. *Genome Biol* **16**, 245, doi:10.1186/s13059-015-0801-3 (2015).
105 You, X. *et al.* Neural circular RNAs are derived from synaptic genes and regulated by development and plasticity. *Nat Neurosci* **18**, 603-610, doi:10.1038/nn.3975 (2015).
106 Zhang, Y. *et al.* Circular RNAs: emerging cancer biomarkers and targets. *J Exp Clin Cancer Res* **36**, 152, doi:10.1186/s13046-017-0624-z (2017).
107 Westholm, J. O. *et al.* Genome-wide analysis of drosophila circular RNAs reveals their structural and sequence properties and age-dependent neural accumulation. *Cell Rep* **9**, 1966-1980, doi:10.1016/j.celrep.2014.10.062 (2014).
108 Gruner, H., Cortes-Lopez, M., Cooper, D. A., Bauer, M. & Miura, P. CircRNA accumulation in the aging mouse brain. *Sci Rep* **6**, 38907, doi:10.1038/srep38907 (2016).

doi:10.6342/NTU202000765

109 Fan, X. *et al.* Single-cell RNA-seq transcriptome analysis of linear and circular RNAs in mouse preimplantation embryos. *Genome Biol* **16**, 148, doi:10.1186/s13059-015-0706-1 (2015).
110 Szabo, L. *et al.* Statistically based splicing detection reveals neural enrichment and tissue-specific induction of circular RNA during human fetal development. *Genome Biol* **16**, 126, doi:10.1186/s13059-015-0690-5 (2015).
111 Guo, J. U., Agarwal, V., Guo, H. & Bartel, D. P. Expanded identification and characterization of mammalian circular RNAs. *Genome Biol* **15**, 409, doi:10.1186/s13059-014-0409-z (2014).
112 Salzman, J., Chen, R. E., Olsen, M. N., Wang, P. L. & Brown, P. O. Cell-type specific features of circular RNA expression. *PLoS Genet* **9**, e1003777, doi:10.1371/journal.pgen.1003777 (2013).
113 Hansen, T. B. *et al.* Natural RNA circles function as efficient microRNA sponges. *Nature* **495**, 384-388, doi:10.1038/nature11993 (2013).
114 Huang, X. *et al.* Circular RNA circERBB2 promotes gallbladder cancer progression by regulating PA2G4-dependent rDNA transcription. *Mol Cancer* **18**, 166, doi:10.1186/s12943-019-1098-8 (2019).
115 Pandey, P. R. *et al.* circSamd4 represses myogenic transcriptional activity of PUR proteins. *Nucleic Acids Res*, doi:10.1093/nar/gkaa035 (2020).
116 Huang, A., Zheng, H., Wu, Z., Chen, M. & Huang, Y. Circular RNA-protein interactions: functions, mechanisms, and identification. *Theranostics* **10**, 3503-3517, doi:10.7150/thno.42174 (2020).
117 Abdelmohsen, K. *et al.* Identification of HuR target circular RNAs uncovers suppression of PABPN1 translation by CircPABPN1. *RNA Biol* **14**, 361-369, doi:10.1080/15476286.2017.1279788 (2017).
118 Yang, Z. G. *et al.* The Circular RNA Interacts with STAT3, Increasing Its Nuclear Translocation and Wound Repair by Modulating Dnmt3a and miR-17 Function. *Mol Ther* **25**, 2062-2074, doi:10.1016/j.ymthe.2017.05.022 (2017).
119 Holdt, L. M. *et al.* Circular non-coding RNA ANRIL modulates ribosomal RNA maturation and atherosclerosis in humans. *Nat Commun* **7**, 12429, doi:10.1038/ncomms12429 (2016).
120 Yang, W., Du, W. W., Li, X., Yee, A. J. & Yang, B. B. Foxo3 activity promoted by non-coding effects of circular RNA and Foxo3 pseudogene in the inhibition of tumor growth and angiogenesis. *Oncogene* **35**, 3919-3931, doi:10.1038/onc.2015.460 (2016).
121 Du, W. W. *et al.* Induction of tumor apoptosis through a circular RNA enhancing Foxo3 activity. *Cell Death Differ* **24**, 357-370, doi:10.1038/cdd.2016.133 (2017).
122 Du, W. W. *et al.* Foxo3 circular RNA promotes cardiac senescence by modulating multiple factors associated with stress and senescence responses. *Eur Heart J* **38**, 1402-1412, doi:10.1093/eurheartj/ehw001 (2017).
123 Zeng, Y. *et al.* A Circular RNA Binds To and Activates AKT Phosphorylation and Nuclear Localization Reducing Apoptosis and Enhancing Cardiac Repair. *Theranostics* **7**, 3842-3855, doi:10.7150/thno.19764 (2017).

doi:10.6342/NTU202000765

124 Legnini, I. *et al.* Circ-ZNF609 Is a Circular RNA that Can Be Translated and Functions in Myogenesis. *Mol Cell* **66**, 22-37 e29, doi:10.1016/j.molcel.2017.02.017 (2017).
125 Yang, Y. *et al.* Novel Role of FBXW7 Circular RNA in Repressing Glioma Tumorigenesis. *J Natl Cancer Inst* **110**, doi:10.1093/jnci/djx166 (2018).
126 Xia, X. *et al.* A novel tumor suppressor protein encoded by circular AKT3 RNA inhibits glioblastoma tumorigenicity by competing with active phosphoinositide-dependent Kinase-1. *Mol Cancer* **18**, 131, doi:10.1186/s12943-019-1056-5 (2019).
127 Zheng, X. *et al.* A novel protein encoded by a circular RNA circPPP1R12A promotes tumor pathogenesis and metastasis of colon cancer via Hippo-YAP signaling. *Mol Cancer* **18**, 47, doi:10.1186/s12943-019-1010-6 (2019).
128 Piwecka, M. *et al.* Loss of a mammalian circular RNA locus causes miRNA deregulation and affects brain function. *Science* **357**, doi:10.1126/science.aam8526 (2017).
129 Hicks, S. D. & Middleton, F. A. A Comparative Review of microRNA Expression Patterns in Autism Spectrum Disorder. *Front Psychiatry* **7**, 176, doi:10.3389/fpsyt.2016.00176 (2016).
130 Han, D. *et al.* Circular RNA circMTO1 Acts as the Sponge of MicroRNA-9 to Suppress Hepatocellular Carcinoma Progression. *Hepatology* **66**, 1151-1164, doi:10.1002/hep.29270 (2017).
131 Wan, L. *et al.* Circular RNA-ITCH Suppresses Lung Cancer Proliferation via Inhibiting the Wnt/beta-Catenin Pathway. *Biomed Res Int* **2016**, 1579490, doi:10.1155/2016/1579490 (2016).
132 Hsiao, K. Y. *et al.* Noncoding Effects of Circular RNA CCDC66 Promote Colon Cancer Growth and Metastasis. *Cancer Res* **77**, 2339-2350, doi:10.1158/0008-5472.CAN-16-1883 (2017).
133 Cheng, Z. A. *et al.* circTP63 functions as a ceRNA to promote lung squamous cell carcinoma progression by upregulating FOXM1. *Nature Communications* **10**, doi:10.1038/s41467-019-11162-4 (2019).
134 Lukiw, W. J. Circular RNA (circRNA) in Alzheimer's disease (AD). *Front Genet* **4**, 307, doi:10.3389/fgene.2013.00307 (2013).
135 Junn, E. *et al.* Repression of alpha-synuclein expression and toxicity by microRNA-7. *Proc Natl Acad Sci U S A* **106**, 13052-13057, doi:10.1073/pnas.0906277106 (2009).
136 Cui, X. *et al.* hsa_circRNA_103636: potential novel diagnostic and therapeutic biomarker in Major depressive disorder. *Biomark Med* **10**, 943-952, doi:10.2217/bmm-2016-0130 (2016).
137 Chen, Y. T. *et al.* Cerebellar degeneration-related antigen: a highly conserved neuroectodermal marker mapped to chromosomes X in human and mouse. *Proc Natl Acad Sci U S A* **87**, 3077-3081 (1990).
138 Zhao, Y., Alexandrov, P. N., Jaber, V. & Lukiw, W. J. Deficiency in the Ubiquitin Conjugating Enzyme UBE2A in Alzheimer's Disease (AD) is Linked to Deficits in a Natural Circular miRNA-7 Sponge (circRNA; ciRS-7). *Genes (Basel)* **7**, doi:10.3390/genes7120116 (2016).

doi:10.6342/NTU202000765

139 Shi, Z. *et al.* The circular RNA ciRS-7 promotes APP and BACE1 degradation in an NF-kappaB-dependent manner. *The FEBS journal* **284**, 1096-1109, doi:10.1111/febs.14045 (2017).
140 Zhou, J., Xiong, Q., Chen, H., Yang, C. & Fan, Y. Identification of the Spinal Expression Profile of Non-coding RNAs Involved in Neuropathic Pain Following Spared Nerve Injury by Sequence Analysis. *Front Mol Neurosci* **10**, 91, doi:10.3389/fnmol.2017.00091 (2017).
141 Chen, B. J. *et al.* Characterization of circular RNAs landscape in multiple system atrophy brain. *J Neurochem* **139**, 485-496, doi:10.1111/jnc.13752 (2016).
142 Song, X. *et al.* Circular RNA profile in gliomas revealed by identification tool UROBORUS. *Nucleic Acids Res* **44**, e87, doi:10.1093/nar/gkw075 (2016).
143 Huang, R. *et al.* Circular RNA HIPK2 regulates astrocyte activation via cooperation of autophagy and ER stress by targeting MIR124-2HG. *Autophagy* **13**, 1722-1741, doi:10.1080/15548627.2017.1356975 (2017).
144 Nan, A. *et al.* A novel regulatory network among LncRpa, CircRar1, MiR-671 and apoptotic genes promotes lead-induced neuronal cell apoptosis. *Archives of Toxicology* **91**, 1671-1684, doi:10.1007/s00204-016-1837-1 (2017).
145 Lin, S. P. *et al.* Circular RNA expression alterations are involved in OGD/R-induced neuron injury. *Biochem Biophys Res Commun* **471**, 52-56, doi:10.1016/j.bbrc.2016.01.183 (2016).
146 Liu, C. *et al.* Screening circular RNA expression patterns following focal cerebral ischemia in mice. *Oncotarget* **8**, 86535-86547, doi:10.18632/oncotarget.21238 (2017).
147 Bai, Y. *et al.* Circular RNA DLGAP4 Ameliorates Ischemic Stroke Outcomes by Targeting miR-143 to Regulate Endothelial-Mesenchymal Transition Associated with Blood-Brain Barrier Integrity. *J Neurosci* **38**, 32-50, doi:10.1523/JNEUROSCI.1348-17.2017 (2018).
148 Han, B. *et al.* Novel insight into circular RNA HECTD1 in astrocyte activation via autophagy by targeting MIR142-TIPARP: implications for cerebral ischemic stroke. *Autophagy* **14**, 1164-1184, doi:10.1080/15548627.2018.1458173 (2018).
149 Szabo, L. & Salzman, J. Detecting circular RNAs: bioinformatic and experimental challenges. *Nat Rev Genet* **17**, 679-692, doi:10.1038/nrg.2016.114 (2016).
150 Chen, I., Chen, C. Y. & Chuang, T. J. Biogenesis, identification, and function of exonic circular RNAs. *Wiley Interdiscip Rev RNA* **6**, 563-579, doi:10.1002/wrna.1294 (2015).
151 Chen, L. *et al.* The bioinformatics toolbox for circRNA discovery and analysis. *Brief Bioinform* (2020).
152 Hansen, T. B., Veno, M. T., Damgaard, C. K. & Kjems, J. Comparison of circular RNA prediction tools. *Nucleic Acids Res* **44**, e58, doi:10.1093/nar/gkv1458 (2016).
153 Chuang, T. J. *et al.* NCLscan: accurate identification of non-co-linear transcripts (fusion, trans-splicing and circular RNA) with a good balance between sensitivity and precision. *Nucleic Acids Res* **44**, e29, doi:10.1093/nar/gkv1013 (2016).

doi:10.6342/NTU202000765

154 Zeng, X., Lin, W., Guo, M. & Zou, Q. A comprehensive overview and evaluation of circular RNA detection tools. *PLoS Comput Biol* **13**, e1005420, doi:10.1371/journal.pcbi.1005420 (2017).
155 Agabian, N. Trans splicing of nuclear pre-mRNAs. *Cell* **61**, 1157-1160, doi:10.1016/0092-8674(90)90674-4 (1990).
156 Cocquet, J., Chong, A., Zhang, G. L. & Veitia, R. A. Reverse transcriptase template switching and false alternative transcripts. *Genomics* **88**, 127-131, doi:10.1016/j.ygeno.2005.12.013 (2006).
157 Yu, C. Y., Liu, H. J., Hung, L. Y., Kuo, H. C. & Chuang, T. J. Is an observed non-co-linear RNA product spliced in trans, in cis or just in vitro? *Nucleic Acids Res* **42**, 9410-9423, doi:10.1093/nar/gku643 (2014).
158 Suzuki, H. & Tsukahara, T. A view of pre-mRNA splicing from RNase R resistant RNAs. *Int J Mol Sci* **15**, 9331-9342, doi:10.3390/ijms15069331 (2014).
159 Schneider, T., Schreiner, S., Preusser, C., Bindereif, A. & Rossbach, O. Northern Blot Analysis of Circular RNAs. *Methods Mol Biol* **1724**, 119-133, doi:10.1007/978-1-4939-7562-4_10 (2018).
160 Willsey, A. J. *et al.* Coexpression networks implicate human midfetal deep cortical projection neurons in the pathogenesis of autism. *Cell* **155**, 997-1007, doi:10.1016/j.cell.2013.10.020 (2013).
161 Parikshak, N. N. *et al.* Integrative functional genomic analyses implicate specific molecular pathways and circuits in autism. *Cell* **155**, 1008-1021, doi:10.1016/j.cell.2013.10.031 (2013).
162 Chen, C. Y. & Chuang, T. J. Comment on "A comprehensive overview and evaluation of circular RNA detection tools". *PLoS computational biology* **15**, e1006158, doi:10.1371/journal.pcbi.1006158 (2019).
163 Chen, C. Y. & Chuang, T. J. NCLcomparator: systematically post-screening non-co-linear transcripts (circular, trans-spliced, or fusion RNAs) identified from various detectors. *BMC Bioinformatics* **20**, 3, doi:10.1186/s12859-018-2589-0 (2019).
164 Glazar, P., Papavasileiou, P. & Rajewsky, N. circBase: a database for circular RNAs. *RNA* **20**, 1666-1670, doi:10.1261/rna.043687.113 (2014).
165 Dong, R., Ma, X. K., Li, G. W. & Yang, L. CIRCpedia v2: An Updated Database for Comprehensive Circular RNA Annotation and Expression Comparison. *Genomics Proteomics Bioinformatics* **16**, 226-233, doi:10.1016/j.gpb.2018.08.001 (2018).
166 Kuhn, R. M., Haussler, D. & Kent, W. J. The UCSC genome browser and associated tools. *Brief Bioinform* **14**, 144-161, doi:10.1093/bib/bbs038 (2013).
167 Dobin, A. *et al.* STAR: ultrafast universal RNA-seq aligner. *Bioinformatics* **29**, 15-21, doi:10.1093/bioinformatics/bts635 (2013).
168 Hansen, K. D., Irizarry, R. A. & Wu, Z. Removing technical variability in RNA-seq data using conditional quantile normalization. *Biostatistics* **13**, 204-216, doi:10.1093/biostatistics/kxr054 (2012).
169 Pinheiro, J., Bates, D., DebRoy, S., Sarkar, D., & Team, R. C. nlme: Linear and Nonlinear Mixed Effects Models. (2019).

doi:10.6342/NTU202000765

170 Langfelder, P. & Horvath, S. WGCNA: an R package for weighted correlation network analysis. *BMC Bioinformatics* **9**, 559, doi:10.1186/1471-2105-9-559 (2008).
171 Shannon, P. *et al.* Cytoscape: a software environment for integrated models of biomolecular interaction networks. *Genome Res* **13**, 2498-2504, doi:10.1101/gr.1239303 (2003).
172 Miranda, K. C. *et al.* A pattern-based method for the identification of MicroRNA binding sites and their corresponding heteroduplexes. *Cell* **126**, 1203-1217, doi:10.1016/j.cell.2006.07.031 (2006).
173 Gascard, P. *et al.* Epigenetic and transcriptional determinants of the human breast. *Nat Commun* **6**, 6351, doi:10.1038/ncomms7351 (2015).
174 Kramer, A., Green, J., Pollard, J., Jr. & Tugendreich, S. Causal analysis approaches in Ingenuity Pathway Analysis. *Bioinformatics* **30**, 523-530, doi:10.1093/bioinformatics/btt703 (2014).
175 Karagkouni, D. *et al.* DIANA-TarBase v8: a decade-long collection of experimentally supported miRNA-gene interactions. *Nucleic acids research* **46**, D239-D245, doi:10.1093/nar/gkx1141 (2018).
176 Agarwal, V., Bell, G. W., Nam, J. W. & Bartel, D. P. Predicting effective microRNA target sites in mammalian mRNAs. *Elife* **4**, e05005, doi:10.7554/eLife.05005 (2015).
177 Wong, N. & Wang, X. miRDB: an online resource for microRNA target prediction and functional annotations. *Nucleic acids research* **43**, D146-152, doi:10.1093/nar/gku1104 (2015).
178 Liu, W. & Wang, X. Prediction of functional microRNA targets by integrative modeling of microRNA binding and target expression data. *Genome biology* **20**, 18, doi:10.1186/s13059-019-1629-z (2019).
179 Fisher, R. A. *Statistical Methods for Research Workers 4th edition*. (London: Oliver and Boyd, 1932).
180 Abrahams, B. S. *et al.* SFARI Gene 2.0: a community-driven knowledgebase for the autism spectrum disorders (ASDs). *Mol Autism* **4**, 36, doi:10.1186/2040-2392-4-36 (2013).
181 Satterstrom, F. K. e. a. Large-scale exome sequencing study implicates both developmental and functional changes in the neurobiology of autism. *bioRxiv*, 484113 [preprint] (2019).
182 Ran, X. *et al.* EpilepsyGene: a genetic resource for genes and mutations related to epilepsy. *Nucleic acids research* **43**, D893-899, doi:10.1093/nar/gku943 (2015).
183 Schizophrenia Working Group of the Psychiatric Genomics, C. Biological insights from 108 schizophrenia-associated genetic loci. *Nature* **511**, 421-427, doi:10.1038/nature13595 (2014).
184 Lango Allen, H. *et al.* Hundreds of variants clustered in genomic loci and biological pathways affect human height. *Nature* **467**, 832-838, doi:10.1038/nature09410 (2010).
185 Wang, P., Zhao, D., Lachman, H. M. & Zheng, D. Enriched expression of genes associated with autism spectrum disorders in human inhibitory neurons. *Transl Psychiatry* **8**, 13, doi:10.1038/s41398-017-0058-6 (2018).

doi:10.6342/NTU202000765

186 Chen, J., Bardes, E. E., Aronow, B. J. & Jegga, A. G. ToppGene Suite for gene list enrichment analysis and candidate gene prioritization. *Nucleic acids research* **37**, W305-311, doi:10.1093/nar/gkp427 (2009).
187 Takahashi, K. & Yamanaka, S. Induction of pluripotent stem cells from mouse embryonic and adult fibroblast cultures by defined factors. *Cell* **126**, 663-676, doi:10.1016/j.cell.2006.07.024 (2006).
188 Donato, R. *et al.* Differential development of neuronal physiological responsiveness in two human neural stem cell lines. *BMC Neurosci* **8**, 36, doi:10.1186/1471-2202-8-36 (2007).
189 Chaerkady, R. *et al.* Temporal analysis of neural differentiation using quantitative proteomics. *J Proteome Res* **8**, 1315-1326, doi:10.1021/pr8006667 (2009).
190 Enright, A. J. *et al.* MicroRNA targets in Drosophila. *Genome Biol* **5**, R1, doi:10.1186/gb-2003-5-1-r1 (2003).
191 Oldham, M. C. *et al.* Functional organization of the transcriptome in human brain. *Nat Neurosci* **11**, 1271-1282, doi:10.1038/nn.2207 (2008).
192 Langfelder, P., Luo, R., Oldham, M. C. & Horvath, S. Is my network module preserved and reproducible? *PLoS computational biology* **7**, e1001057, doi:10.1371/journal.pcbi.1001057 (2011).
193 Mariani, J. *et al.* FOXG1-Dependent Dysregulation of GABA/Glutamate Neuron Differentiation in Autism Spectrum Disorders. *Cell* **162**, 375-390, doi:10.1016/j.cell.2015.06.034 (2015).
194 Darnell, J. C. *et al.* FMRP stalls ribosomal translocation on mRNAs linked to synaptic function and autism. *Cell* **146**, 247-261, doi:10.1016/j.cell.2011.06.013 (2011).
195 Mukherjee, N. *et al.* Integrative Regulatory Mapping Indicates that the RNA-Binding Protein HuR Couples Pre-mRNA Processing and mRNA Stability. *Mol Cell* **43**, 327-339, doi:10.1016/j.molcel.2011.06.007 (2011).
196 Weyn-Vanhentenryck, S. M. *et al.* HITS-CLIP and integrative modeling define the Rbfox splicing-regulatory network linked to brain development and autism. *Cell Rep* **6**, 1139-1152, doi:10.1016/j.celrep.2014.02.005 (2014).
197 Kraushar, M. L. *et al.* Temporally defined neocortical translation and polysome assembly are determined by the RNA-binding protein Hu antigen R. *P Natl Acad Sci USA* **111**, E3815-E3824, doi:10.1073/pnas.1408305111 (2014).
198 Popovitchenko, T. *et al.* The RNA binding protein HuR determines the differential translation of autism-associated FoxP subfamily members in the developing neocortex. *Sci Rep* **6**, 28998, doi:10.1038/srep28998 (2016).
199 Nakanishi, M. *et al.* Functional significance of rare neuroligin 1 variants found in autism. *Plos Genetics* **13**, doi:10.1371/journal.pgen.1006940 (2017).
200 Memczak, S., Papavasileiou, P., Peters, O. & Rajewsky, N. Identification and Characterization of Circular RNAs As a New Class of Putative Biomarkers in Human Blood. *Plos One* **10**, doi:10.1371/journal.pone.0141214 (2015).
201 Bahn, J. H. *et al.* The landscape of microRNA, Piwi-interacting RNA, and circular RNA in human saliva. *Clin Chem* **61**, 221-230, doi:10.1373/clinchem.2014.230433 (2015).

doi:10.6342/NTU202000765

202 Zhang, Z., Yang, T. & Xiao, J. Circular RNAs: Promising Biomarkers for Human Diseases. *EBioMedicine* **34**, 267-274, doi:10.1016/j.ebiom.2018.07.036 (2018).
203 Lasda, E. & Parker, R. Circular RNAs Co-Precipitate with Extracellular Vesicles: A Possible Mechanism for circRNA Clearance. *Plos One* **11**, e0148407, doi:10.1371/journal.pone.0148407 (2016).
204 Li, J. *et al.* Circular RNA IARS (circ-IARS) secreted by pancreatic cancer cells and located within exosomes regulates endothelial monolayer permeability to promote tumor metastasis. *J Exp Clin Canc Res* **37**, doi:10.1186/s13046-018-0822-3 (2018).
205 Jin, H. Y. *et al.* Transfection of microRNA Mimics Should Be Used with Caution. *Frontiers in Genetics* **6**, doi:10.3389/fgene.2015.00340 (2015).
206 Gabrielli, A. P., Manzardo, A. M. & Butler, M. G. GeneAnalytics Pathways and Profiling of Shared Autism and Cancer Genes. *Int J Mol Sci* **20**, doi:10.3390/ijms20051166 (2019).
207 Wen, Y., Alshikho, M. J. & Herbert, M. R. Pathway Network Analyses for Autism Reveal Multisystem Involvement, Major Overlaps with Other Diseases and Convergence upon MAPK and Calcium Signaling. *Plos One* **11**, doi:10.1371/journal.pone.0153329 (2016).
208 Xiong, W. *et al.* Microarray Analysis of Circular RNA Expression Profile Associated with 5-Fluorouracil-Based Chemoradiation Resistance in Colorectal Cancer Cells. *Biomed Res Int* **2017**, 8421614, doi:10.1155/2017/8421614 (2017).
209 Wang, K. *et al.* Exome sequencing identifies frequent mutation of ARID1A in molecular subtypes of gastric cancer. *Nat Genet* **43**, 1219-1223, doi:10.1038/ng.982 (2011).
210 Wiegand, K. C. *et al.* ARID1A mutations in endometriosis-associated ovarian carcinomas. *N Engl J Med* **363**, 1532-1543, doi:10.1056/NEJMoa1008433 (2010).
211 Li, L., Li, M., Jiang, Z. & Wang, X. ARID1A Mutations Are Associated with Increased Immune Activity in Gastrointestinal Cancer. *Cells* **8**, doi:10.3390/cells8070678 (2019).

doi:10.6342/NTU202000765